Dense matter from lattice QCD (?)

Color-superconducting strange quark matter

Surface
- Hydrogen/Helium plasma
- Iron nuclei

Outer Crust
- Atomic nuclei
- Electron gas

Inner Crust
- Heavy atomic nuclei
- Relativistic electron gas
- Superfluid neutrons

Outer Core
- Neutrons, superconducting protons
- Electrons, muons

Inner Core
- Neutrons, protons, electrons, muons
- Hyperons (Σ, Λ, Ξ)
- Boson (π, K) condensates
- Deconfined (u,d,s) quarks / color-superconducting quark matter

Radius ~ 10 to 14 km, Mass ~ 1 to 2 M_{sun}

F. Weber (SDSU, 2010)
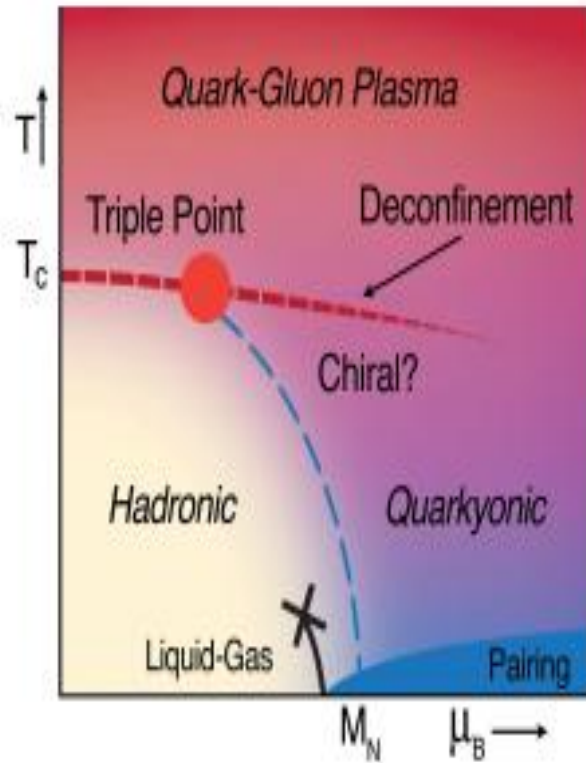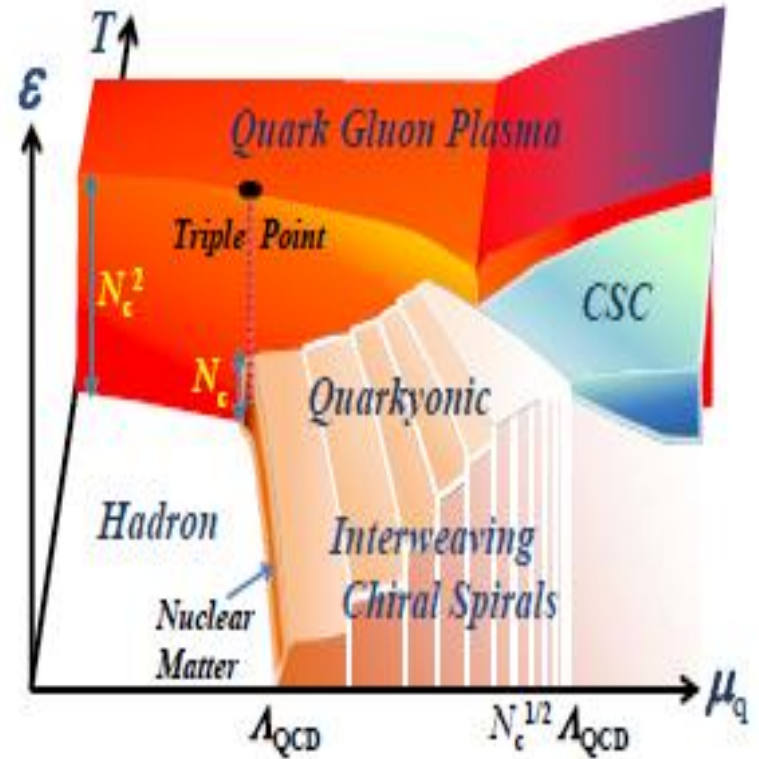
Maria Paola Lombardo

GGI Firenze
March 2014

The phases of strong interactions

Andronic et al 2010

Tojo et al 2011

..and the experimental programs

First
proposal:

Cabibbo
and Parisi,
1975

The Phases of QCD

LHC

RHIC

NICA /FAIR / RHIC II

Quark-Gluon Plasma

Temperature

Early Universe

~170 MeV

Crossover

Critical Point

Hadron Gas

Color Superconductor

Vacuum

Nuclear Matter

Neutron Stars

0 MeV

0 MeV

900 MeV

Baryon Chemical Potential

US NSAC Long RangePlan (adapted)
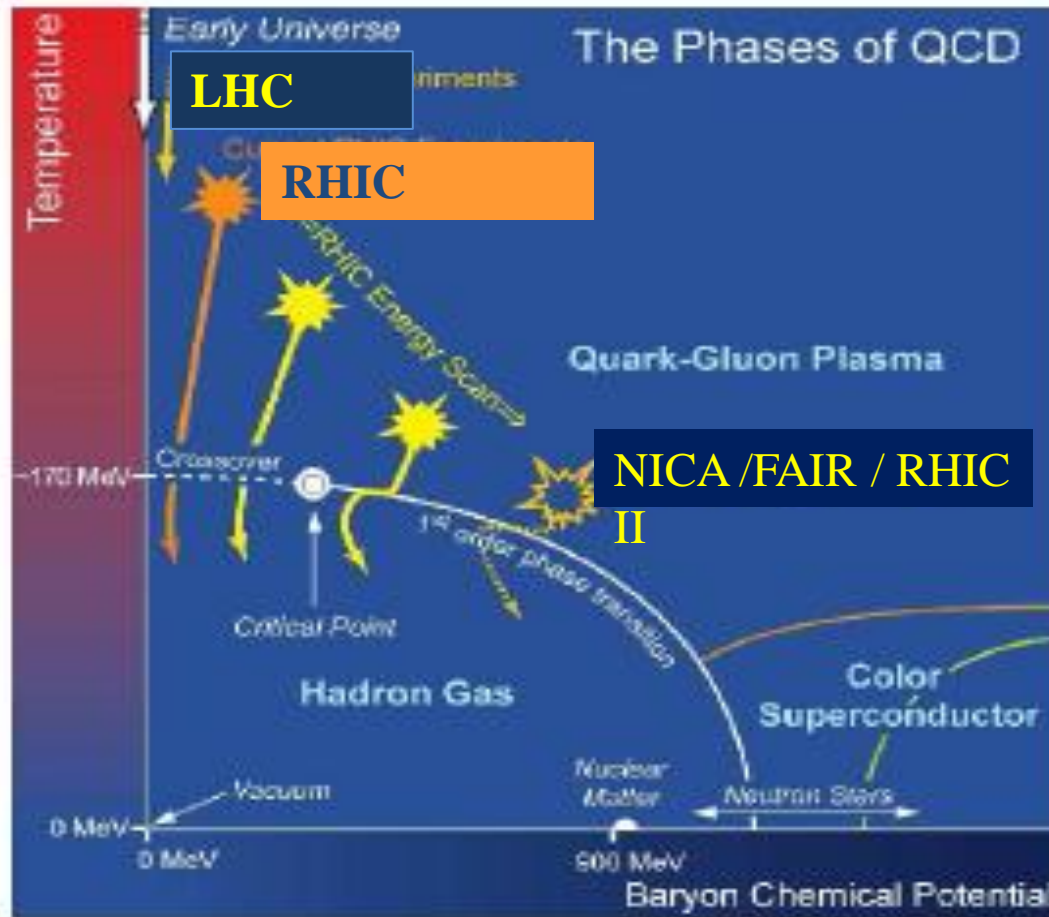
(Dense) matter on the lattice

QCD, and the lattice

Few body physics , nuclear potential and the nuclear equation of state

EoS and condensates from first principles in QCD-like models I: fermionic models

EoS and condensates from first principles in QCD-like models II: two color QCD

Overview of methods and results in QCD

The critical point of QCD

Fundamental theory of strong interactions

QCD, AND THE LATTICE

LATTICE QCD ALLOWS FIRST PRINCIPLES CALCULATIONS FROM THE QCD LAGRANGIAN

$$\mathcal{L} = \mathcal{L}_{YM} + \bar{\psi}(i\gamma_\mu D_\mu + m + \mu\gamma_0)\psi$$

We can tune physical parameter, as in real experiments: baryon chemical potential, temperature, isospin chemical potential, strangeness,..

We can also play with number of color and number of flavor.

We can address phenomenological issues as well as theoretical questions.

QCD

$$Z(V, T, \mu) = \int \mathcal{D}A_\nu \mathcal{D}\bar{\psi} \mathcal{D}\psi \, e^{-S_E(V,T,\mu)}$$

$$S_E(V, T, \mu) \equiv S_G(V, T) \; + \; S_F(V, T, \mu)$$

$$S_G(V, T) = \int_0^{1/T} dx_0 \int_V d^3x \, \frac{1}{2} \text{Tr} \, F_{\mu\nu} F_{\mu\nu}$$

$$S_F(V, T, \mu) = \int_0^{1/T} dx_0 \int_V d^3x \sum_{f=1}^{n_f} \bar{\psi}_f \left(\gamma_\mu [\partial_\mu - ig A_\mu] + m_f - \mu \gamma_0 \right) \psi_f.$$

..on the lattice

$$\beta S_G = \beta \sum_{\substack{n \\ 0 \le \mu < \nu \le 3}} W^{(1,1)}_{n,\mu\nu} \implies \int \mathrm{d}^4 x \, \mathcal{L}_E + \mathcal{O}(a^2)$$

$$W^{(1,1)}_{n,\mu\nu} = 1 - \frac{1}{3} \mathrm{Re} \, \square_{n,\mu\nu} \equiv \mathrm{Re} \, \mathrm{Tr} \, U_{n,\mu} U_{n+\hat{\mu},\nu} U^\dagger_{n+\hat{\nu},\mu} U^\dagger_{n,\nu}$$

$$= \frac{g^2 a^4}{2} F^a_{\mu\nu} F^a_{\mu\nu} + \mathcal{O}(a^6) \quad .$$

$$U_{x,\mu} = \mathrm{P} \exp\left(ig \int_x^{x+\hat{\mu} a} \mathrm{d}x^\mu \, A_\mu(x) \right)$$

$$S_F^{KS} = \sum_{nm} \bar{\chi}_n Q^{KS}_{nm} \chi_m$$

$$Q^{KS}_{nm}(m_q, \tilde{\mu}) = \frac{1}{2} \sum_{\mu=1}^{3} (-1)^{n_0 + \ldots + n_{\mu-1}} \left(\delta_{n+\hat{\mu},m} U_{n,\mu} - \delta_{n,m+\hat{\mu}} U^\dagger_{m,\mu} \right)$$

$$+ \frac{1}{2} \left(\delta_{n+\hat{0},m} U_{n,0} \, \mathrm{e}^{\tilde{\mu}} - \delta_{n,m+\hat{0}} U^\dagger_{m,0} \right) \mathrm{e}^{-\tilde{\mu}} + \delta_{nm} m_q$$

Designing a simulation

$$Z(N_\sigma, N_\tau, \beta, m_q, \tilde{\mu}) = \int \prod_{n\nu} dU_{n,\nu} (\det Q^{KS}(m_q, \tilde{\mu}))^{n_f/4} e^{-\beta S_G}$$
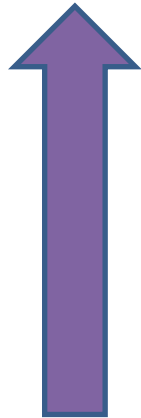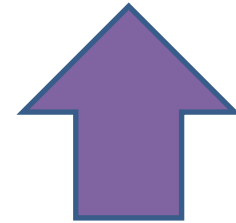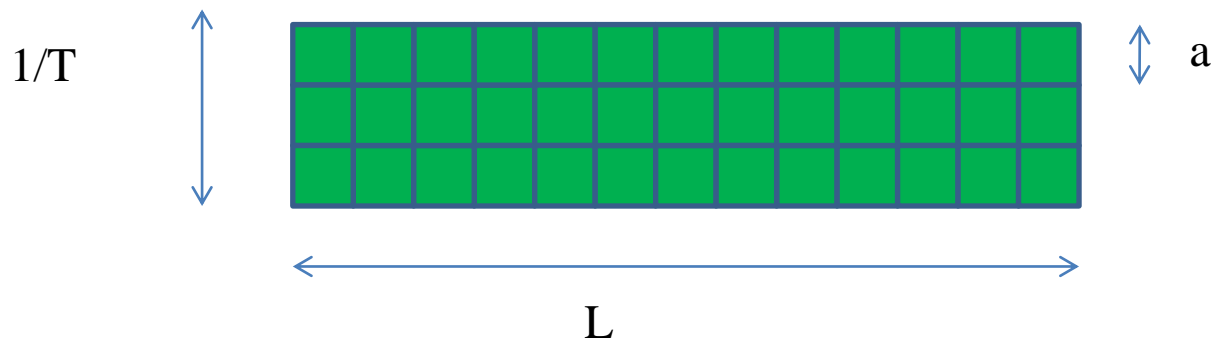
Choice of the discretization

Input parameters

Dimensional transmutation

$$a\Lambda_L \simeq (6b_0/\beta)^{-b_1/2b_0^2} e^{-\beta/12b_0}$$

$$\beta = 6/g^2$$

1/T

a

L

..and check of the continuumlimit

COMPUTATIONAL SCHEMES

$$\mathcal{Z} = \int d\phi d\bar{\psi} dU\, e^{-S(\phi,\bar{\psi},U)}; \quad S(\phi,\bar{\psi},U) = \int_0^{1/T} dt \int d^d x \mathcal{L}(\phi,\bar{\psi}U)$$

$$\mathcal{L}_{QCD} = \mathcal{L}_{YM} + \bar{\psi}(i\gamma_\mu D_\mu + m)\psi + \mu\bar{\psi}\gamma_0\psi$$

Two options:

1. Integrate out gluons first:

$$\mathcal{Z}(T,\mu,\bar{\psi},\psi,U) \simeq \mathcal{Z}(T,\mu,\bar{\psi},\psi) \rightarrow$$

effective approximate fermion models

2. Integrate out fermions exactly as S is bilinear in ψ, $\bar{\psi}$
$$S = S_{YM}(U) + \bar{\psi}M(U)\psi$$

$$\mathcal{Z}(T,\mu,U) = \int dU\, e^{-(S_{YM}(U)-log(detM))} \rightarrow$$

starting point for numerical calculations

The strong coupling expansion

A long history..
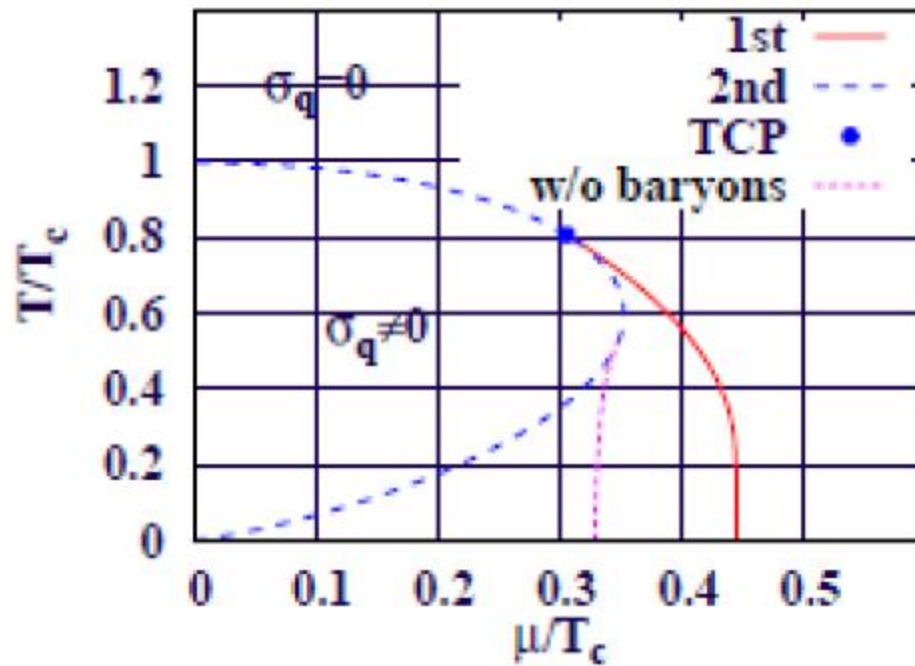
Kawamoto, Miura, Onishi 2007

IMPORTANCE SAMPLING AND THE POSITIVITY ISSUE

$$\mathcal{Z}(T, \mu, U) = \int dU e^{-(S_{YM}(U) - log(\det M))}$$

### $\det M > 0 \rightarrow$ IMPORTANCE SAMPLING
MONTECARLO SIMULATIONS

To assess sign problem consider $M^\dagger(\mu_B) = -M(-\mu_B)$

- $\mu = 0 \rightarrow \det M$ is real
  Particles-antiparticles symmetry : MC Simulations OK

- Imaginary $\mu \neq 0 \rightarrow \det M$ is real
  (Real) Particles-antiparticles symmetry : MC Simulations OK

- Real $\mu \neq 0$ Particles-antiparticles asymmetry
  $\rightarrow \det M$ is complex in QCD

QCD with a real baryon chemical potential:
use information from the accessible region

$$Real\mu = 0, Im\mu \neq 0$$

Option 2 : Integrate over fermions and ..
The mπ/2 barrier
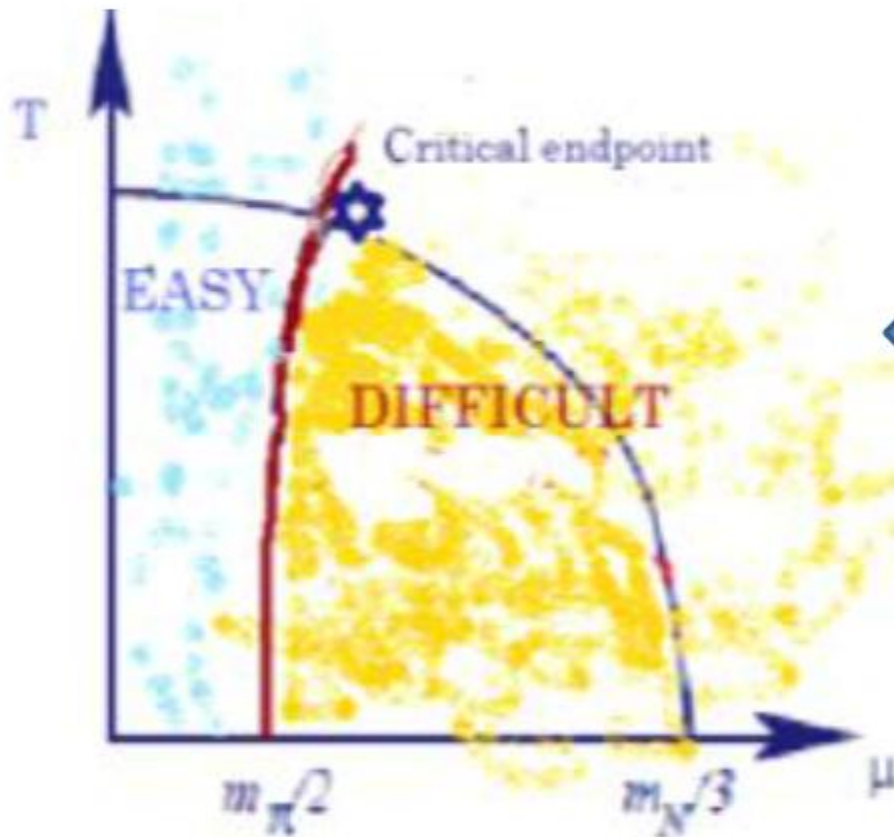
Summary
Of our
efforts!!

FEW BODY RESULTS

$$(m_h/m_\Omega)_{lat} / (m_h/m_\Omega)_{exp} - 1$$

Wuppertal-
Budapest
2013
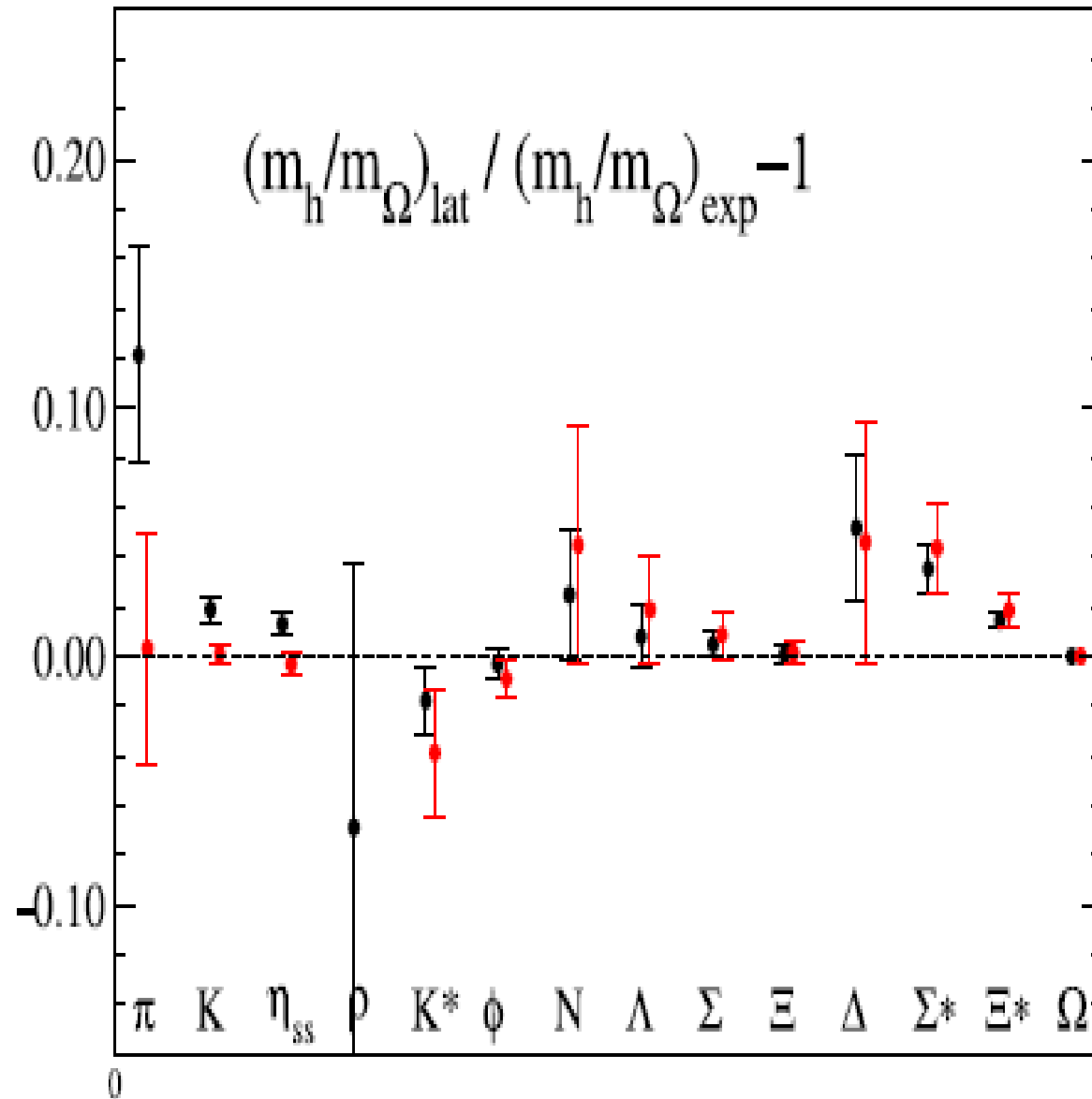
What is the status now (2012)?

$$M_N[\text{MeV}] \simeq 800 + m_\pi$$

$$m_\pi \simeq 758 \text{ MeV}$$

$$m_\pi \simeq 174 \text{ MeV}$$

Legend:
- ★ physical
- LHPC 2008
- χQCD 2012
- RBC: Preliminary DSDR
- RBC: $a^{-1} = 1.75(3)$ GeV
- RBC: $a^{-1} = 2.31(4)$ GeV
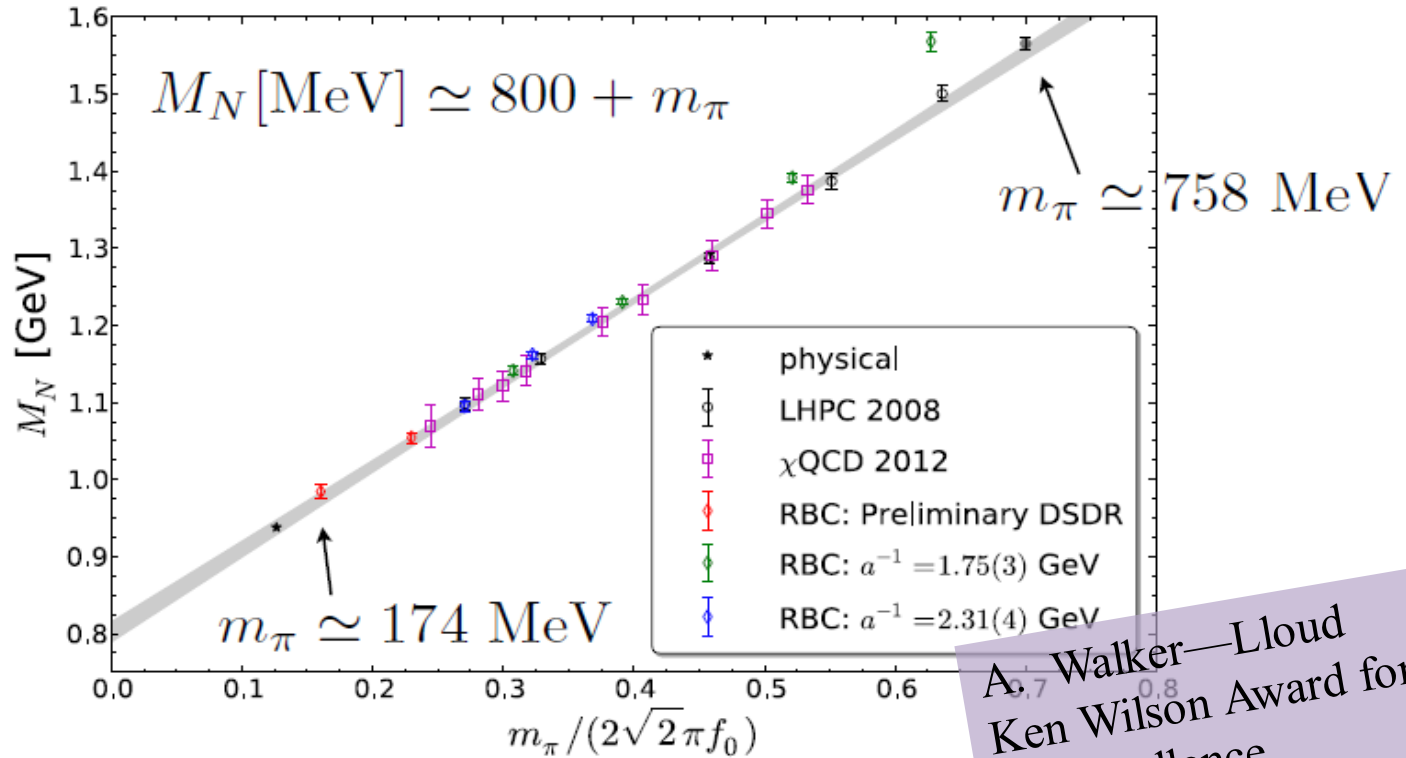
Taking this seriously yields

$$\sigma_{\pi N} = 67 \pm 4 \text{ MeV}$$

I am not advocating this as a good model for QCD!

A. Walker—Lloud
Ken Wilson Award for excellence
In Lattice Field Theory—
Talk at Lattice2013

NNLO $- m_\pi^4$, with $g_A = 1.2(1)$, $g_{\Delta N} = 1.5(3)$
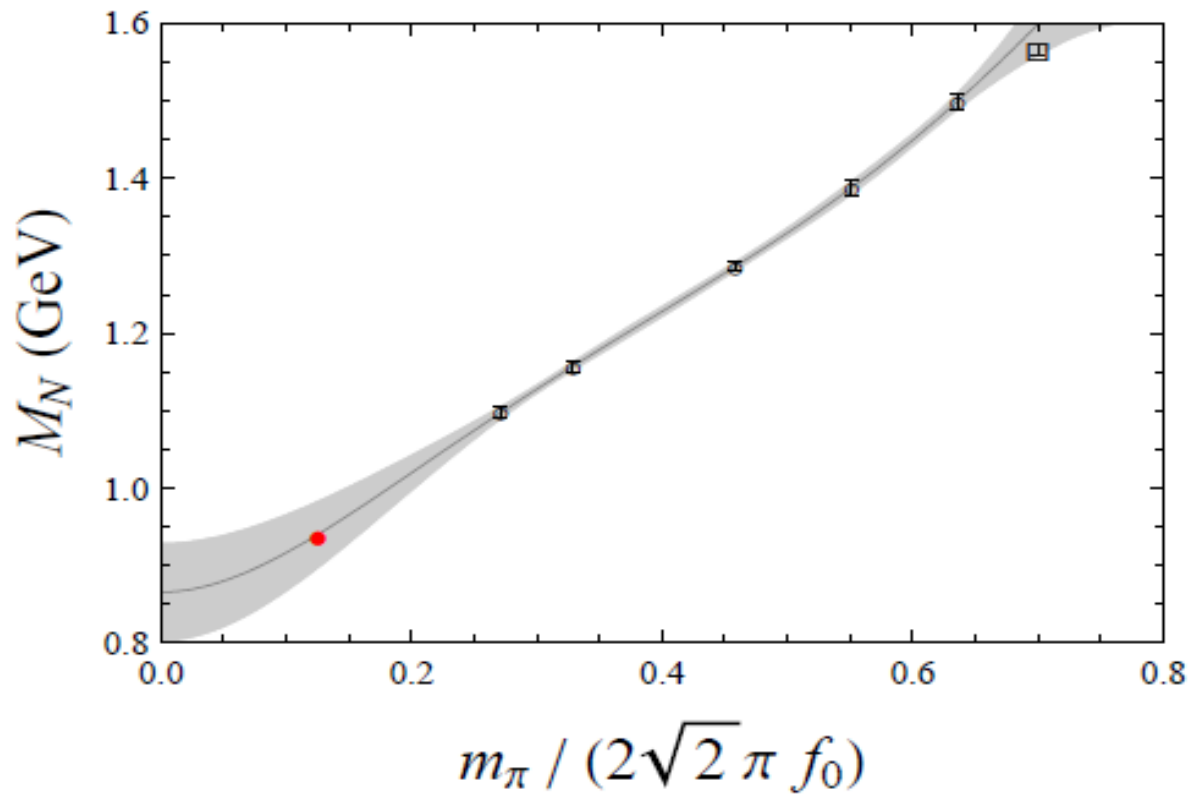
H dibaryon

$$|H\rangle = -\sqrt{\frac{1}{8}}|\Lambda\Lambda\rangle + \sqrt{\frac{3}{8}}|\Sigma\Sigma\rangle + \sqrt{\frac{4}{8}}|N\Xi\rangle.$$
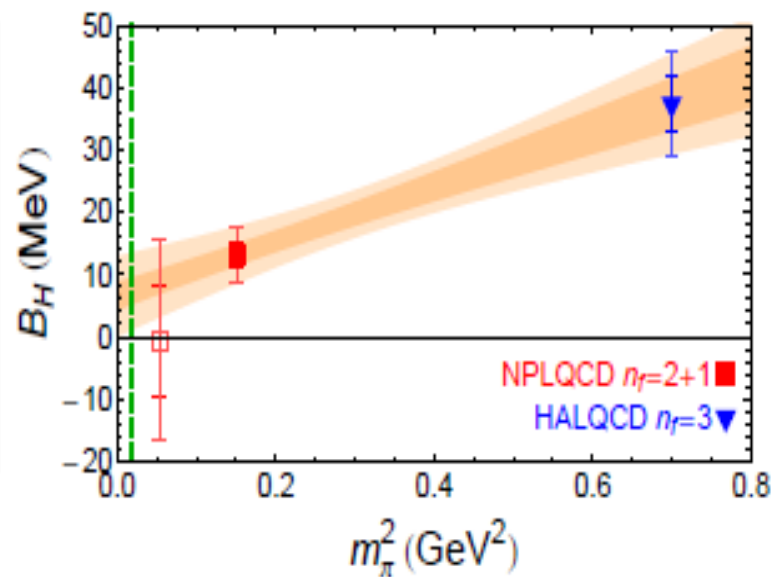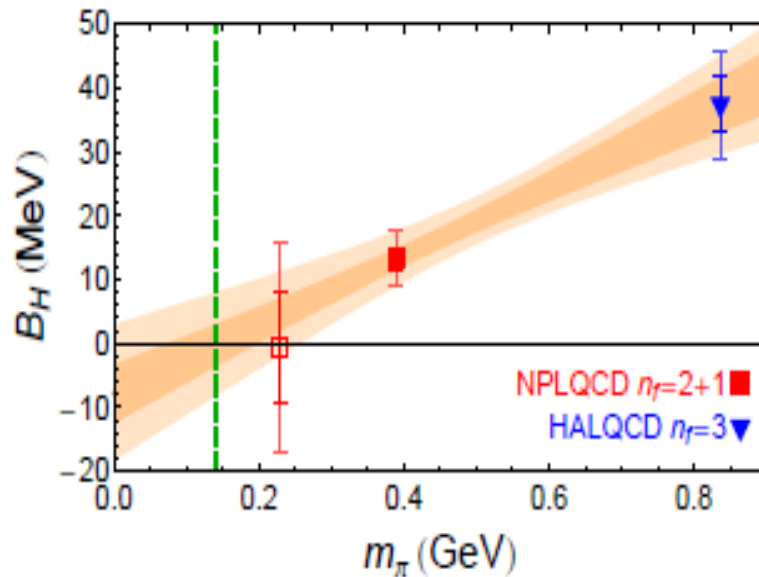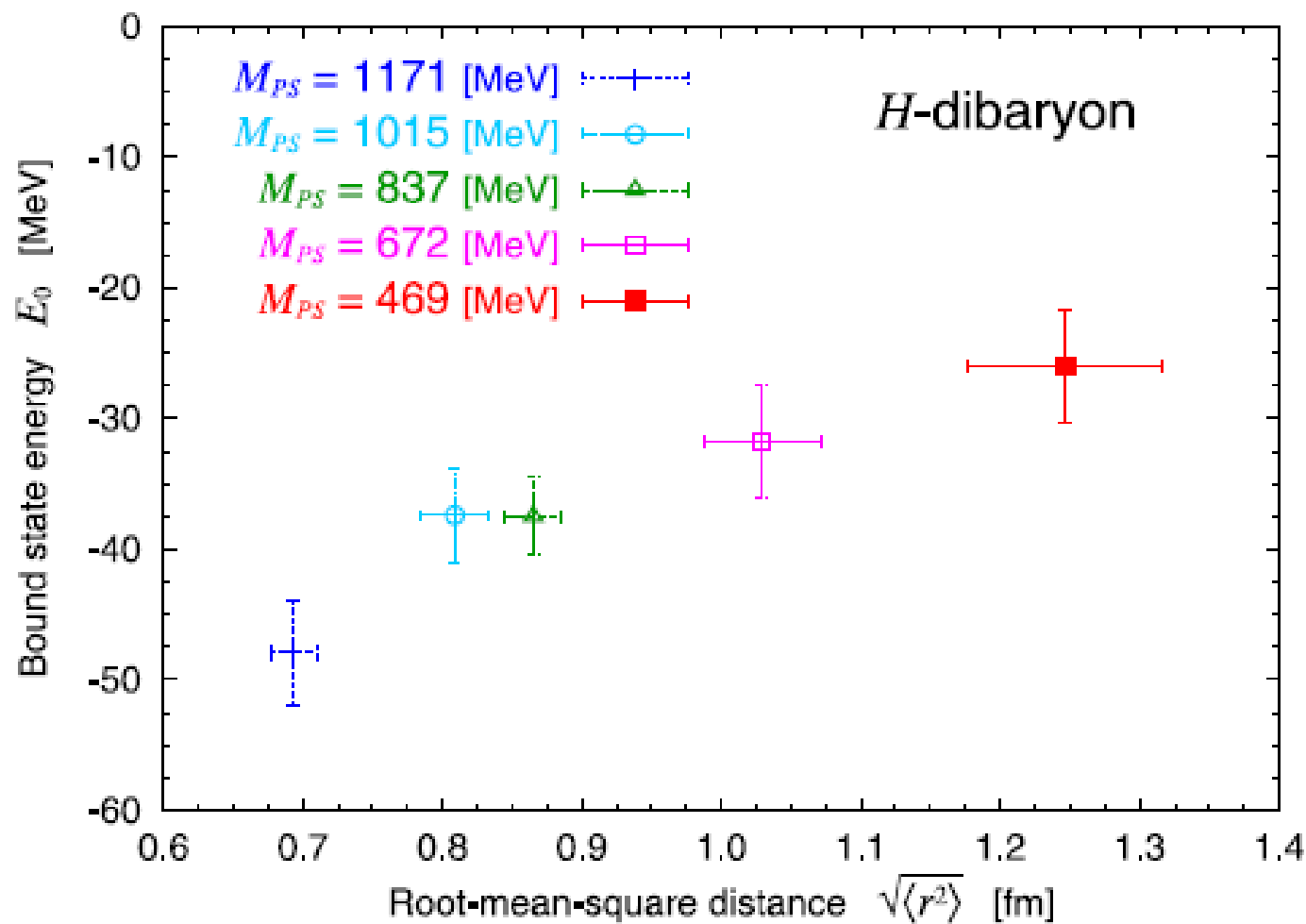
# Nuclear force from Lattice QCD

- Phenomenological NN forces have 20—40 fitting parameters. For hyperon—nucleon and nucleon—nucleon a factor 3 more

- However in QCD all interactions are controlled only by the scale parameter and the physical quark masses

- NN potentials are determined from the equal time Nambu-Bethe-Salpeter wave function

Wave function, Schroedinger equation and potential

$$\psi_n(r) = \langle 0 | N(x+r) N(x) | E_n \rangle,$$

$$(k_n^2 + \nabla^2) \psi_n(r) \equiv m_N \int U(r, r') \psi_n(r') \, dr'.$$

S. Aoki et al. (HAL QCD Collaboration),
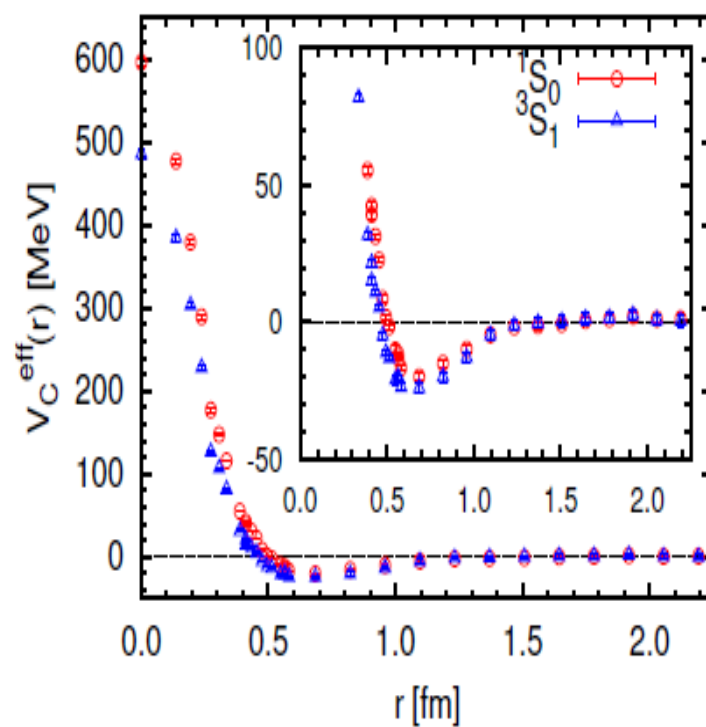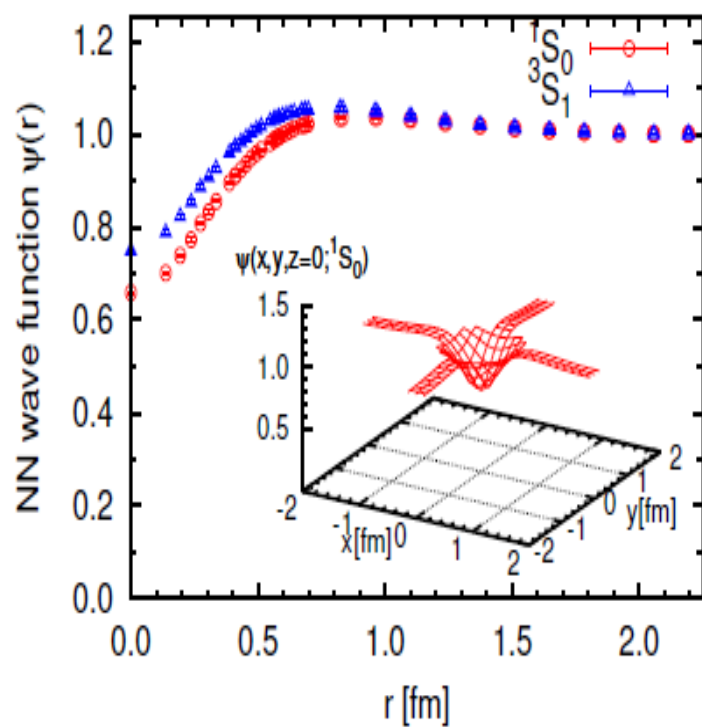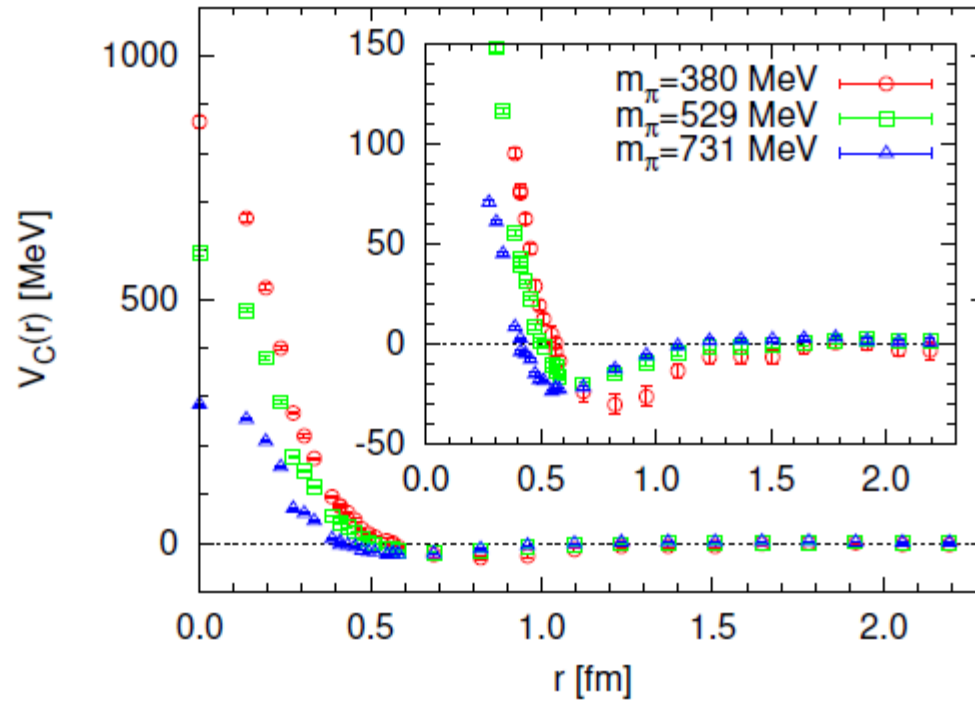
The central potentials for the spin-singlet channel from the orbital A_1^+
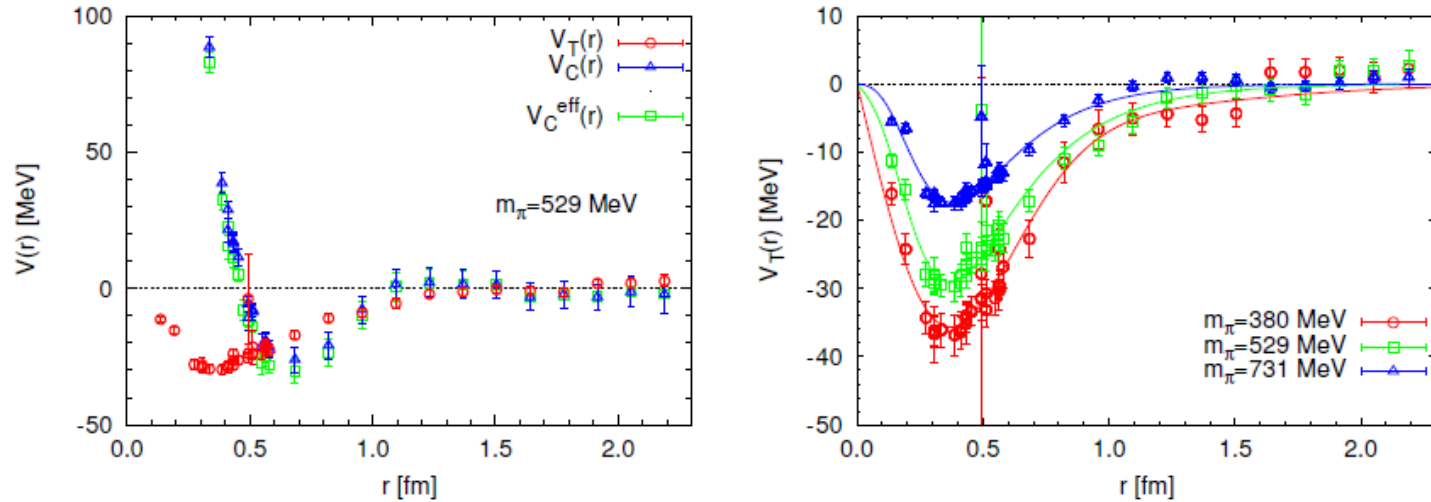
Fits to phenomenological form

Fig. 5. (Left) The central potential $V_C(r)^{(1,0)}$ and the tensor potential $V_T(r)$ obtained from the $J^P = T_1^+$ NBS wave function, together with the effective central potential $V_C^{\mathrm{eff}}(r)^{(1,0)}$, at $m_\pi \simeq 529$ MeV. (Right) Pion mass dependence of the tensor potential. The lines are the four-parameter fit using one-pion-exchange + one-rho-exchange with Gaussian form factor.

$$V_T(r) = b_1(1 - e^{-b_2 r^2})^2 \left(1 + \frac{3}{m_\rho r} + \frac{3}{(m_\rho r)^2}\right) \frac{e^{-m_\rho r}}{r}$$

$$+ b_3(1 - e^{-b_4 r^2})^2 \left(1 + \frac{3}{m_\pi r} + \frac{3}{(m_\pi r)^2}\right) \frac{e^{-m_\pi r}}{r},$$

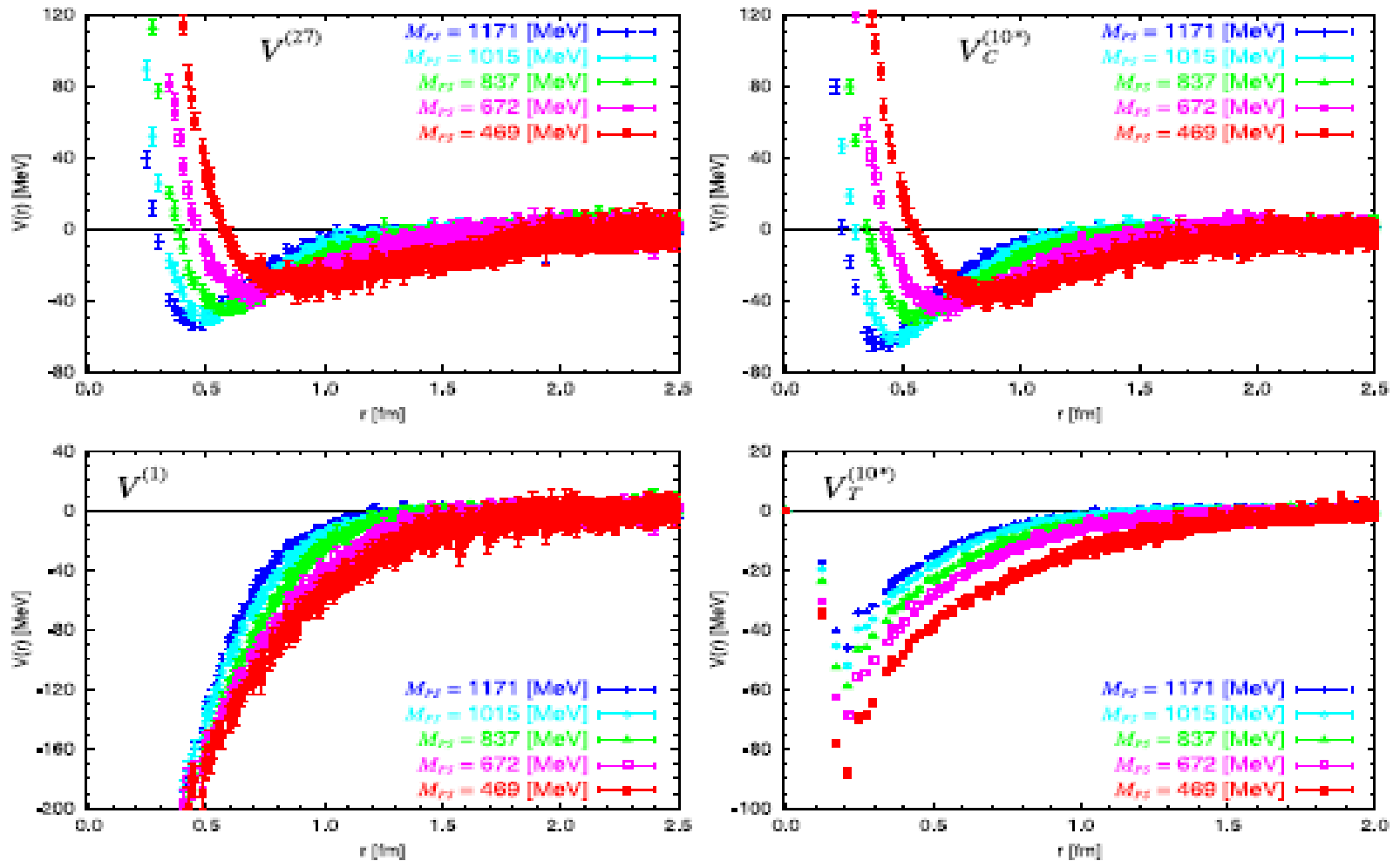# Overview of the results

Fig. 2. Quark mass dependences of baryon–baryon potentials in the flavor SU(3) limit.

Three nucleon forces

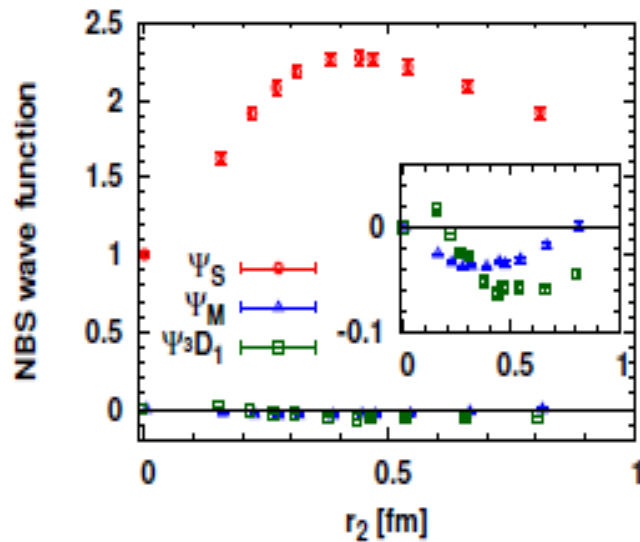Fig. 21. 3N wave functions at $(t - t_0)/a = 8$. Circle (red), triangle (blue), square (green) points denote ψ_S, ψ_M, ψ_{3D_1}, respectively.
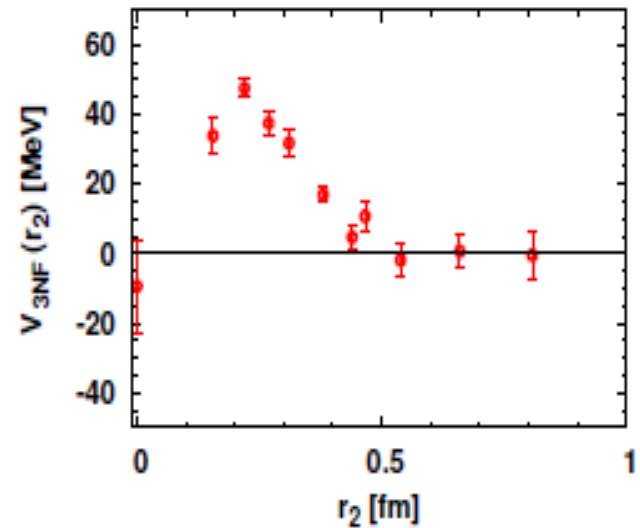

Fig. 22. The effective scalar-isoscalar 3NF in the triton channel with the linear setup obtained at $(t - t_0)/a = 8$. r_2 is the distance between the center and edge in the linear setup.

The short distance repulsion among baryons

Aoki, Balog, Weisz 2013

The wave function at short distance

$$\varphi_E(\vec{r}) \approx \sum_k D_k(\vec{r}) \langle 0|\mathcal{O}_k(\vec{0}, 0)|BB, E\rangle_{\text{in}}.$$

$$D_k(\vec{r}) \approx \lambda(r)^{-\nu_k} d_k,$$

Diverges at r = 0 if $\nu_1 > 0$
Vanishes at r = 0 if $\nu_1 < 0$

$\lambda(r)$ is the 2-loop running coupling defined by

$$\frac{1}{\lambda} + \kappa \ln \lambda = \ln \frac{r_*}{r}, \quad r \ll r_*$$

Implies for the short distance potential

$$V(r) \approx -\frac{\nu_1}{m_N r^2 \left(\ln \frac{r_*}{r}\right)}$$

Attractive if $\nu_1 > 0$
Repulsive if $\nu_1 < 0$

In some cases a mismatch was observed between the sign of the potential and these estimates, indicating that the asymptotic behaviour has not been reached yet on the lattice

Equation of State for Nucleonic Matter and its Quark Mass Dependence from the Nuclear Force in Lattice QCD

Takashi Inoue[1], Sinya Aoki[2,3], Takumi Doi[4], Tetsuo Hatsuda[4,5],
Yoichi Ikeda[4], Noriyoshi Ishii[3], Keiko Murano[4], Hidekatsu Nemura[3], Kenji Sasaki[3]
(HAL QCD Collaboration)

[1] Nihon University, College of Bioresource Sciences, Kanagawa 252-0880, Japan
[2] Yukawa Institute for Theoretical Physics, Kyoto University, Kyoto 606-8502, Japan
[3] Center for Computational Sciences, University of Tsukuba, Ibaraki 305-8571, Japan
[4] Theoretical Research Division, Nishina Center, RIKEN, Saitama 351-0198, Japan
[5] Kavli IPMU (WPI), The University of Tokyo, Chiba 277-8583, Japan

Quark mass dependence of the equation of state (EOS) for nucleonic matter is investigated, on the basis of the Brueckner-Hartree-Fock method with the nucleon-nucleon interaction extracted from lattice QCD simulations. We observe saturation of nuclear matter at the lightest available quark mass corresponding to the pseudoscalar meson mass $\simeq 469$ MeV. Mass-radius relation of the neutron stars is also studied with the EOS for neutron-star matter from the same nuclear force in lattice QCD. We observe that the EOS becomes stiffer and thus the maximum mass of neutron star increases as the quark mass decreases toward the physical point.

September 2013

EoS from lattice nuclear forces

Input : NN potentials from zero strangeness sector in flavor SU(3) QCD
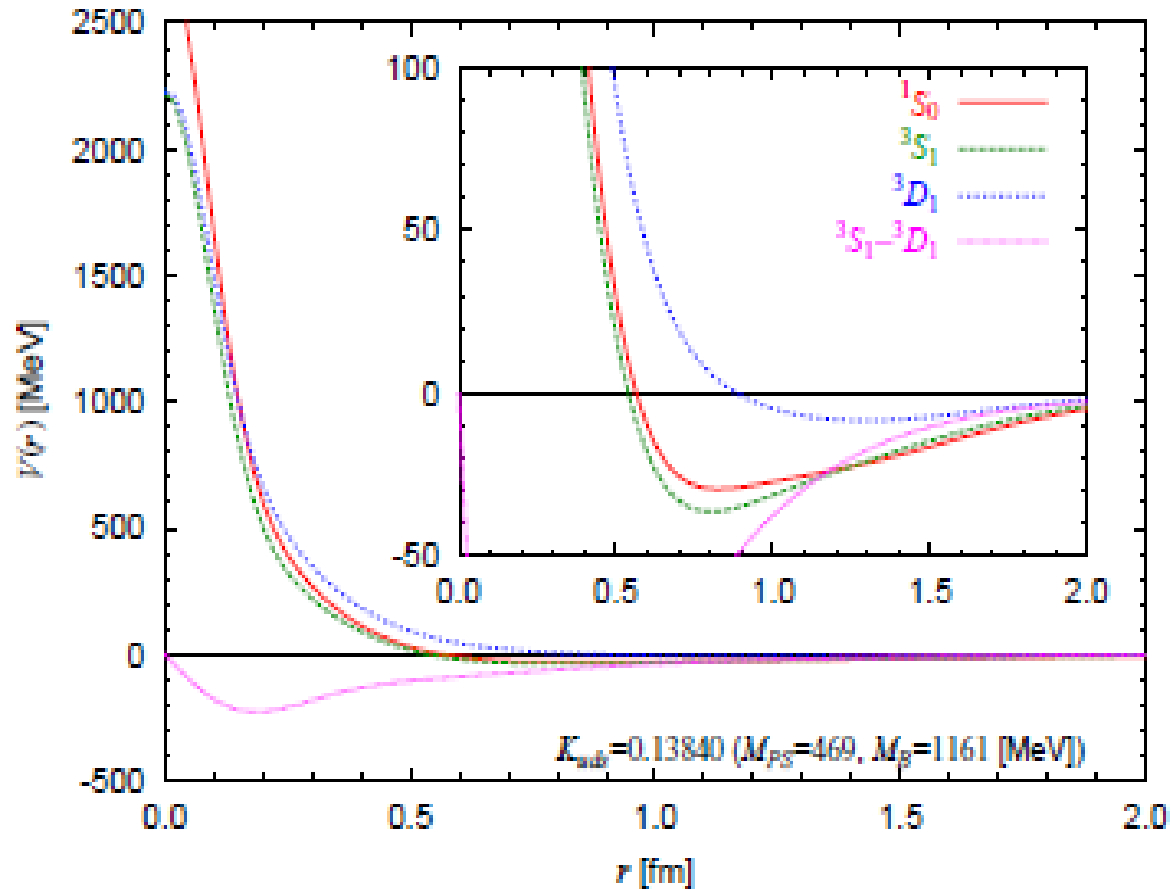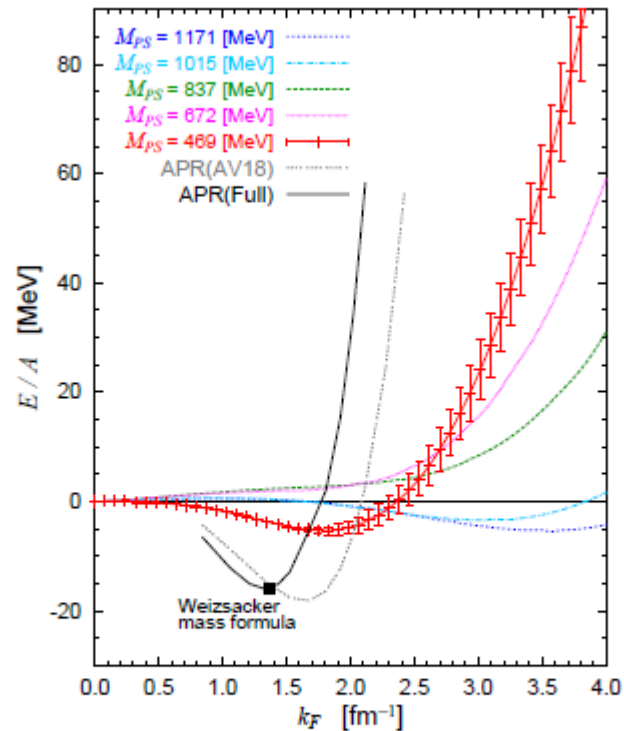
Ground state energies

FIG. 3: Ground state energy per nucleon (E/A) for symmetric nuclear matter as a function of k_F obtained by the BHF theory with the NN potential from lattice QCD. Filled square indicates the minimum of the energy obtained by the
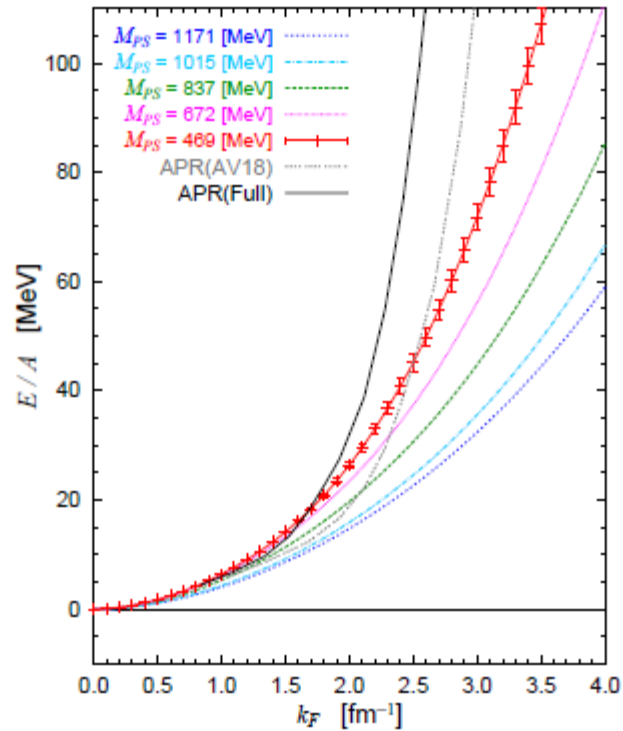
Ground state energies

FIG. 4: Ground state energy per neutron for the pure neutron matter as a function of the Fermi momentum. Details of the calculation are the same as Fig. 3.
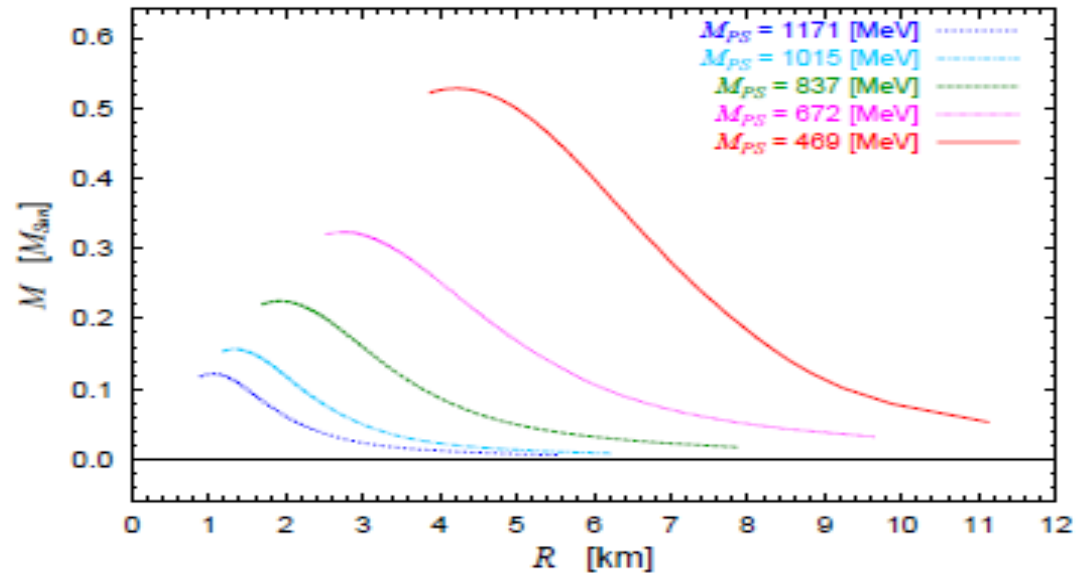
Mass-radius relation

FIG. 5: Mass-radius relation of the neutron star. Neutron-star matter consists of n, p, e^-, and μ^- with charge neutrality and chemical equilibrium. EOS for the nucleons is obtained by an interpolation between Fig. 3 and Fig. 4 under the parabolic approximation.

Equation of State for Nucleonic Matter and its Quark Mass Dependence from the Nuclear Force in Lattice QCD

Takashi Inoue[1], Sinya Aoki[2,3], Takumi Doi[4], Tetsuo Hatsuda[4,5],
Yoichi Ikeda[4], Noriyoshi Ishii[3], Keiko Murano[4], Hidekatsu Nemura[3], Kenji Sasaki[3]

(HAL QCD Collaboration)

[1]Nihon University, College of Bioresource Sciences, Kanagawa 252-0880, Japan
[2]Yukawa Institute for Theoretical Physics, Kyoto University, Kyoto 606-8502, Japan
[3]Center for Computational Sciences, University of Tsukuba, Ibaraki 305-8571, Japan
[4]Theoretical Research Division, Nishina Center, RIKEN, Saitama 351-0198, Japan
[5]Kavli IPMU (WPI), The University of Tokyo, Chiba 277-8583, Japan

Quark mass dependence of the equation of state (EOS) for nucleonic matter is investigated, on the basis of the Brueckner-Hartree-Fock method with the nucleon-nucleon interaction extracted from lattice QCD simulations. We observe saturation of nuclear matter at the lightest available quark mass corresponding to the pseudoscalar meson mass $\simeq 469$ MeV. Mass-radius relation of the neutron stars is also studied with the EOS for neutron-star matter from the same nuclear force in lattice QCD. We observe that the EOS becomes stiffer and thus the maximum mass of neutron star increases as the quark mass decreases toward the physical point.

The equation of state (EOS) for hadronic matter is a key quantity for understanding the physics of compact stars and explosive phenomena in astrophysics. From the observational point of view, recent reports on massive neutron stars put stringent constraints on the EOS [1]. In the future, neutrinos from core-collapsed supernovae and gravitational waves from neutron star mergers will give further constraints on the EOS [2, 3]. From the theoretical point of view, various approaches to calculate the EOS have been pursued so far, e.g. the Brueckner-Bethe-Goldstone theory [4], the quantum Monte Carlo simulations [5], and the chiral effective theories [6, 7]. Although they provide reasonable descriptions of the nuclear matter at low density, it is still beyond the scope of these approaches to answer the fundamental questions such as the quark-mass (m_q) dependence of the nuclear saturation property and the maximum mass of neutron stars. These questions can only be answered by many-body techniques with hadronic interactions obtained by lattice QCD simulations for different m_q.

The purpose of this Letter is to make a first exploratory study for the nuclear and neutron matter EOS by combining the Brueckner-Hartree-Fock (BHF) many-body theory with the nuclear force obtained from lattice QCD simulations. In particular we study how the saturation develops in nuclear matter and how the mass-radius relation of the neutron star changes as a function of m_q: Such m_q dependence of the EOS gives us useful information on the physics of strongly interacting nucleons, even though the values of m_q in this study are still away from the physical one. In addition, it is certainly important to establish a direct connection between lattice QCD and the physics of the nucleonic matter.

The nuclear force which we adopt in this Letter is taken from the zero-strangeness sector of the octet-

TABLE I: M_{PS}, M_V and M_B denote hadron masses corresponding to the pseudoscalar meson, vector meson and octet baryon, respectively, with the $SU(3)$ symmetric hopping parameter κ_{uds} [9]. Trajectory length N_{traj} and number of configurations N_{cfg} are also shown.

κ_{uds}	M_{PS} [MeV]	M_V [MeV]	M_B [MeV]	N_{cfg} / N_{traj}
0.13660	1170.9(7)	1510.4(0.9)	2274(2)	420 / 4200
0.13710	1015.2(6)	1360.6(1.1)	2031(2)	360 / 3600
0.13760	836.5(5)	1188.9(0.9)	1749(1)	480 / 4800
0.13800	672.3(6)	1027.6(1.0)	1484(2)	360 / 3600
0.13840	468.6(7)	829.2(1.5)	1161(2)	720 / 3600

baryon potentials in the flavor-$SU(3)$ limit calculated on the lattice [8, 9], where the renormalization group improved Iwasaki gauge action and the nonperturbatively improved Wilson quark action were employed on a $32^3 \times 32$ lattice with the lattice spacing $a = 0.121(2)$ fm. The potentials were derived from the imaginary-time Nambu-Bethe-Salpeter wave functions by the HAL QCD method [10–12], at the quark masses corresponding to the pseudoscalar meson masses (M_{PS}) ranging between 469 and 1171 MeV. Shown together in Table I are the vector meson mass (M_V) and the baryon mass (M_B) for these quark masses.

In Fig. 1, we show the NN potentials obtained from fits to the lattice data in S and D-waves at $M_{PS} \simeq 469$ MeV. These potentials share common features with phenomenological potentials, i.e., a strong repulsive core at short distance and the attractive pocket at intermediate distance, so that the $^1S_0$ phase shift in Fig. 2 shows qualitatively similar behavior with the experimental data [9]. While the phase shift in the $^3S_1$ channel shows stronger attraction at low energies than that of the

Dense Matter from First Principles

I.

QCD-like models and the strong coupling expansion : condensates, equation of state, search for exotic phases

II.

QCD, and its critical point

Observables and EoS

$$\mathcal{Z} = Tr\hat{\rho}$$

$$\hat{\rho} = e^{-(H-\mu\hat{N})/T}$$

$$< O > = TrO\hat{\rho}/\mathcal{Z}$$

$$P = T\frac{\partial ln\mathcal{Z}}{\partial V}$$

$$N = T\frac{\partial ln\mathcal{Z}}{\partial \mu}$$

$$S = \frac{\partial T ln\mathcal{Z}}{\partial T}$$

$$E = -PV + TS + \mu N$$

FERMIONIC MODELS

2+1 Gross-Neveu model

$$\mathcal{L} = \sum_{j=1}^{N_f} \left[\bar{\psi}^{(j)} \not{\partial} \, \psi^{(j)} - \frac{g^2}{2N_f} (\bar{\psi}^{(j)} \psi^{(j)})^2 \right].$$

Z_2 chiral symmetry is $\psi \mapsto \gamma_5 \psi, \ \bar{\psi} \mapsto -\bar{\psi}\gamma_5$
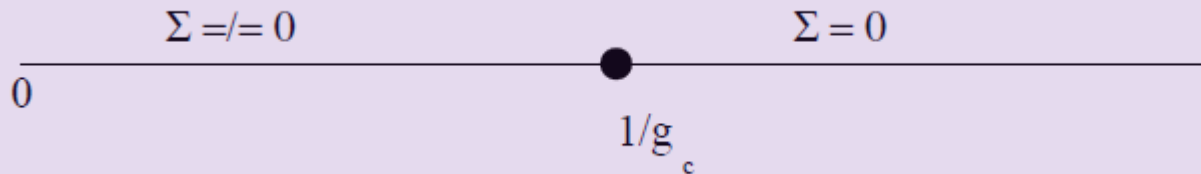
Phase diagram in ordinary conditions

GN model on the continuum and on the lattice

$$\mathcal{L} = \sum_{j=1}^{N_f} \left[\bar{\psi}^{(j)} \slashed{\partial} \psi^{(j)} + \sigma \bar{\psi}^{(j)} \psi^{(j)} \right] + \frac{N_f}{2g^2} \sigma^2$$

$$S = \sum_{i=1}^{N_f/2} \left(\sum_{x,y} \bar{\chi}_i(x) \mathcal{M}_{x,y} \chi_i(y) + \frac{1}{8} \sum_x \bar{\chi}_i(x) \chi_i(x) \sum_{<\tilde{x},x>} \sigma(\tilde{x}) \right) + \frac{N_f}{4g^2} \sum_{\tilde{x}} \sigma^2(\tilde{x}),$$

$$\mathcal{M}_{x,y} = \frac{1}{2} \left[\delta_{y,x+\hat{0}} e^{\mu} - \delta_{y,x-\hat{0}} e^{-\mu} \right] + \frac{1}{2} \sum_{\nu=1,2} \eta_\nu(x) \left[\delta_{y,x+\hat{\nu}} - \delta_{y,x-\hat{\nu}} \right]$$

$$-< \bar{\psi}\psi > = \frac{1}{V} \mathrm{tr} S_F = \frac{1}{V} < \mathrm{tr} M^{-1} >,$$

$$< \epsilon > = -\frac{1}{V_s} \frac{\partial \ln Z}{\partial \beta} = \frac{1}{V} \mathrm{tr} \partial_0 \gamma_0 S_F = \frac{1}{2V} < \sum_x e^{\mu} M^{-1}_{x,x+\hat{0}} - e^{-\mu} M^{-1}_{x,x-\hat{0}} >,$$

$$< n > = -\frac{1}{V_s \beta} \frac{\partial \ln Z}{\partial \mu} = \frac{1}{V} \mathrm{tr} \gamma_0 S_F = \frac{1}{2V} < \sum_x e^{\mu} M^{-1}_{x,x+\hat{0}} + e^{-\mu} M^{-1}_{x,x-\hat{0}} >.$$

Mean field solution vs lattice results

$$\Sigma_0 - \Sigma = T \left(\ln(1 + e^{-\beta(\Sigma-\mu)}) + \ln(1 + e^{-\beta(\Sigma+\mu)}) \right).$$

Set $\Sigma=0$ and obtain the critical line

$$1 - \frac{\mu}{\Sigma_0} = 2\frac{T}{\Sigma_0} \ln(1 + e^{-\beta\mu})$$

Note for T=0 μ—independence till $\mu c = \Sigma_0$
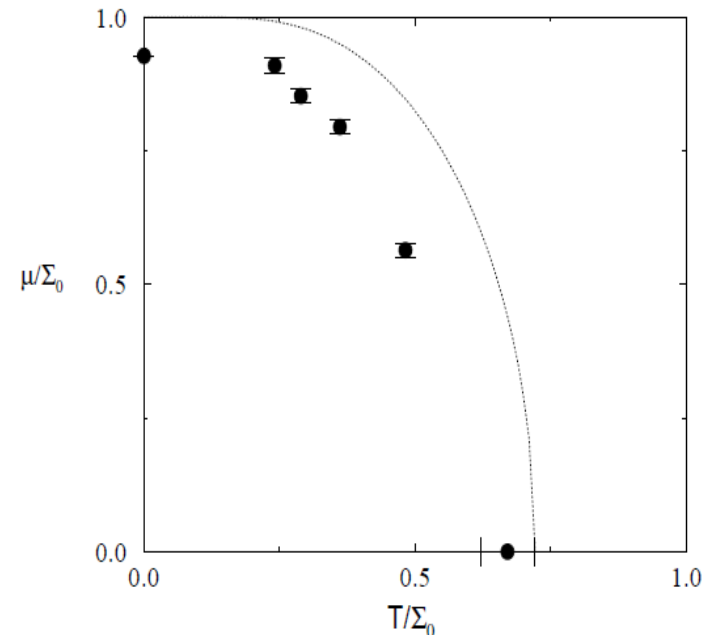
The Phase Diagram of 2+1 GN model : mean field and exact

Hands, Kocic, Kogut 1993
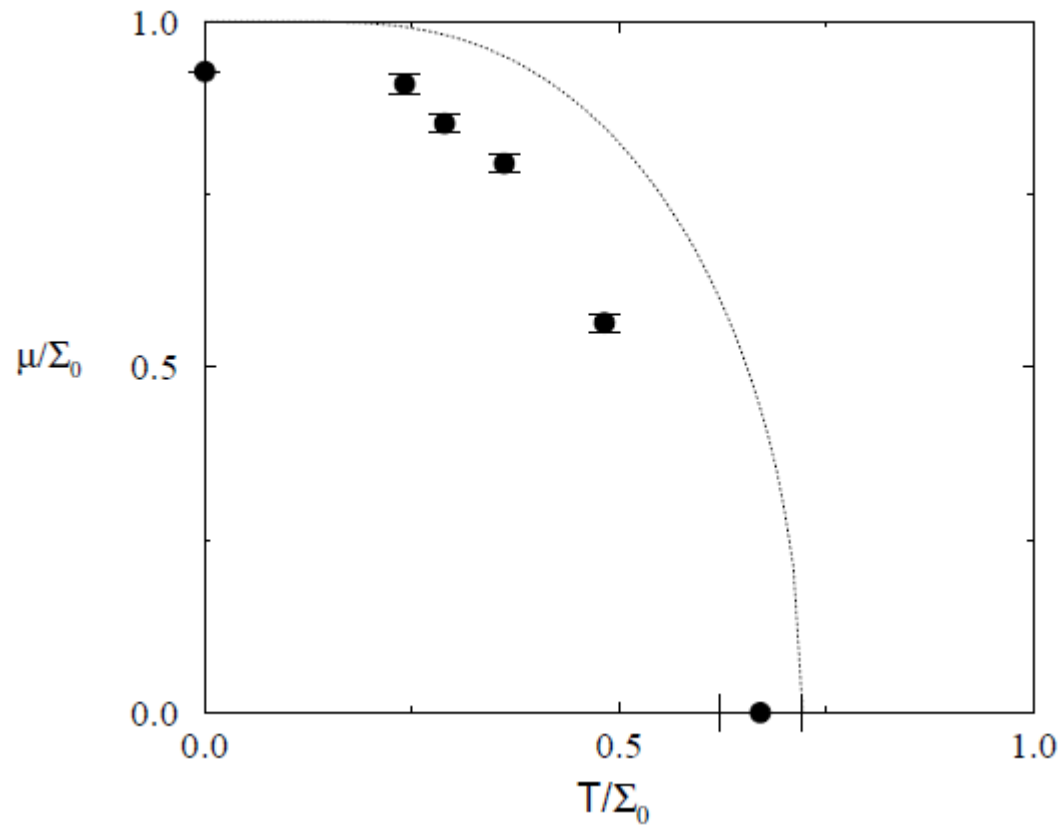
Condensate and EOS in NJL 3+1

Hands and Walters 2003
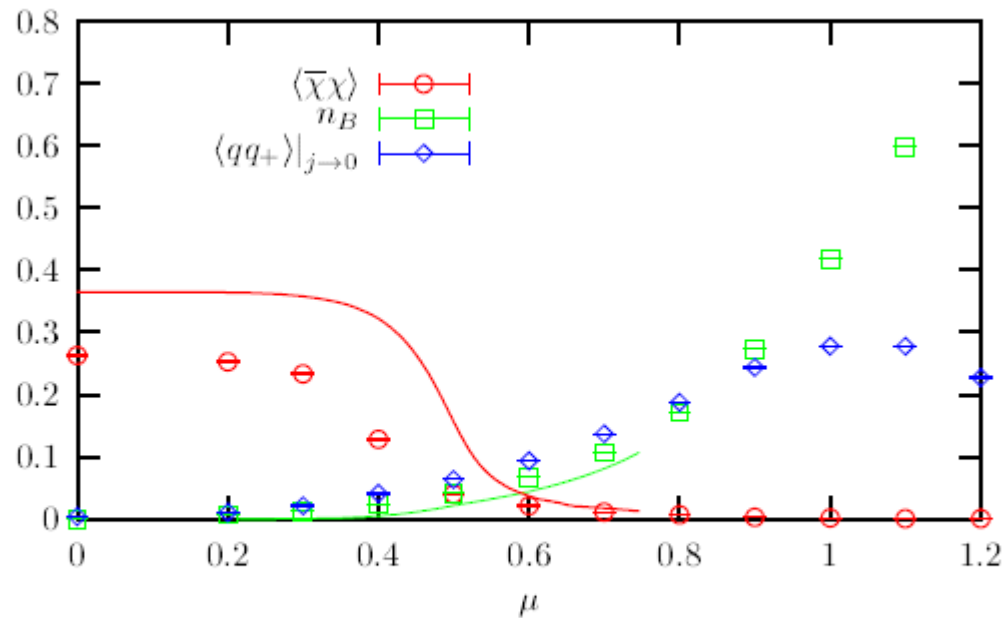
Figure 1. Chiral condensate $\langle \bar{\chi}\chi \rangle$, baryon density, and diquark condensate as functions of μ, showing both large-N_c solution (solid curve) and simulation results (points).

Diquark condensation

$$\langle qq_\pm \rangle = \frac{1}{V} \frac{\partial \ln Z}{\partial j_\pm}$$

$$\lim_{j_+ \to 0} \langle qq_+ \rangle \neq 0$$

if $U(1)_B$ broken
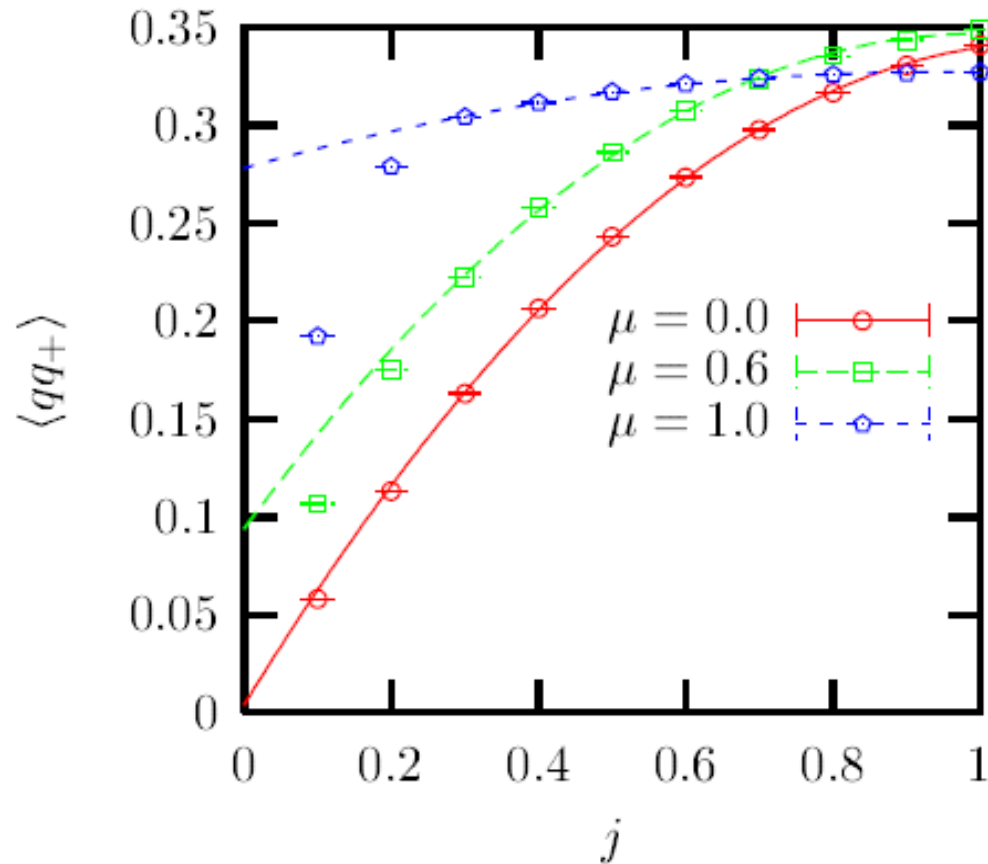
From QCD to four fermion models

$$S = -1/2 \sum_x \sum_{j=1}^{3} \eta_j(x)[\bar{\chi}(x)U_j(x)\chi(x+j) - \bar{\chi}(x+j)U_j^\dagger(x)\chi(x)]$$

$$-1/2 \sum_x \eta_0(x)[\bar{\chi}(x)U_0(x)\chi(x+0) - \bar{\chi}(x+0)U_0^\dagger(x)\chi(x)]$$

$$-1/3 \sum_x 6/g^2 \sum_{\mu,\nu=1}^{4} [1 - reTrU_{\mu\nu}(x)]$$

$$+\sum_x m\bar{\chi}\chi$$

Lattice QCD action with staggered fermions

From QCD to four fermion models

Cfr Lectures by Massimo Mannarelli

$$S = -1/2 \sum_x \sum_{j=1}^{3} \eta_j(x)[\bar{\chi}(x)U_j(x)\chi(x+j) - \bar{\chi}(x+j)U_j^\dagger(x)\chi(x)]$$

$$-1/2 \sum_x \eta_0(x)[\bar{\chi}(x)U_0(x)\chi(x+0) - \bar{\chi}(x+0)U_0^\dagger(x)\chi(x)]$$

$$-1/3 \sum_x 6/g^2 \sum_{\mu,\nu=1}^{4} [1 - reTrU_{\mu\nu}(x)]$$

$$+\sum_x m\bar{\chi}\chi$$

Gauge part disappears
in the infinite coupling
limit

From QCD to four fermion models

$$S = -1/2 \sum_x \sum_{j=1}^{3} \eta_j(x)[\bar{\chi}(x)U_j(x)\chi(x+j) - \bar{\chi}(x+j)U_j^{\dagger}(x)\chi(x)]$$

$$-1/2 \sum_x \eta_0(x)[\bar{\chi}(x)U_0(x)\chi(x+0) - \bar{\chi}(x+0)U_0^{\dagger}(x)\chi(x)]$$

$$-1/3 \sum_x 6/g^2 \sum_{\mu,\nu=1}^{4} [1 - reTrU_{\mu\nu}(x)]$$

$$+\sum_x m\bar{\chi}\chi$$

Gauge part disappears in the infinite coupling limit

Meson operators

$$Z = \int \prod_{timelinks} dU_t d\bar{\chi} d\chi \, e^{-1/4N \sum_{<x,y>} \bar{\chi}(x)\chi(x)\bar{\chi}(y)\chi(y)} e^{-S_t}$$

Sketch of the calculations (T,μ=0)

1) Bosonization

$$Z \simeq \int d\sigma \; exp[-\tfrac{N_c}{4}d\sigma^2 + \tfrac{d}{2}\sigma\overline{\chi}^b(x)\chi^b(x)]$$

2) Mean field

$$\sigma(x) \simeq \sigma(x + \hat{\mu}) = \sigma = <\overline{\chi}\chi>$$

$$\int d[\overline{\chi}\chi]exp[\sigma\overline{\chi}^b(x)\chi^b(x)] = \sigma^{N_c}$$

$$Z = \int d\sigma \; exp[-N_c(\tfrac{d}{4}\sigma^2 - ln\sigma)]$$

$$V(\sigma)$$

$$V(\sigma)$$

**Spontaneous chiral
symmetry breaking
(T=0)**
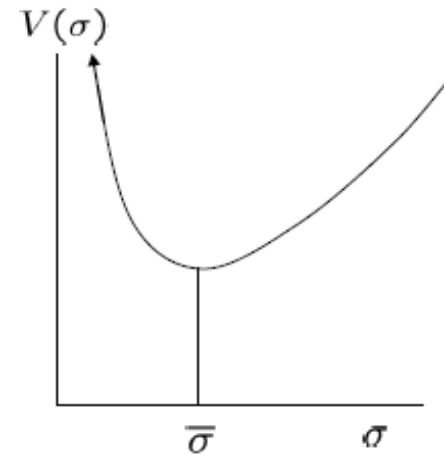
NK-Smit ('81)
Kuberg-stern-Morel-Napoly-Petersson('81)

Results from the strong coupling expansion for finite T and μ
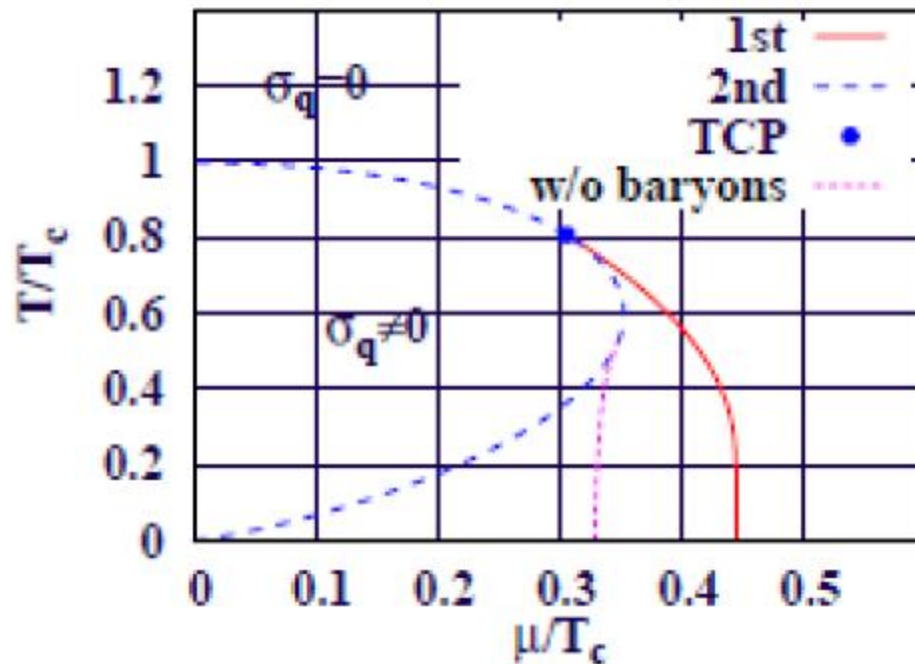
Kawamoto,
Miura, Onishi
2007

The Strong Coupling Expansion
approaching the continuum limit

Phase Diagram Evolution with Increasing $\beta = 2N_c/g^2$
Next-to-Leading Order of $1/g^2$ Expansion
K. Miura, T-Z. Nakano, A. Ohnishi and N. Kawamoto
Phys. Rev. D 80 (2009), 074034.
Courtesy Kohtaroh Miura
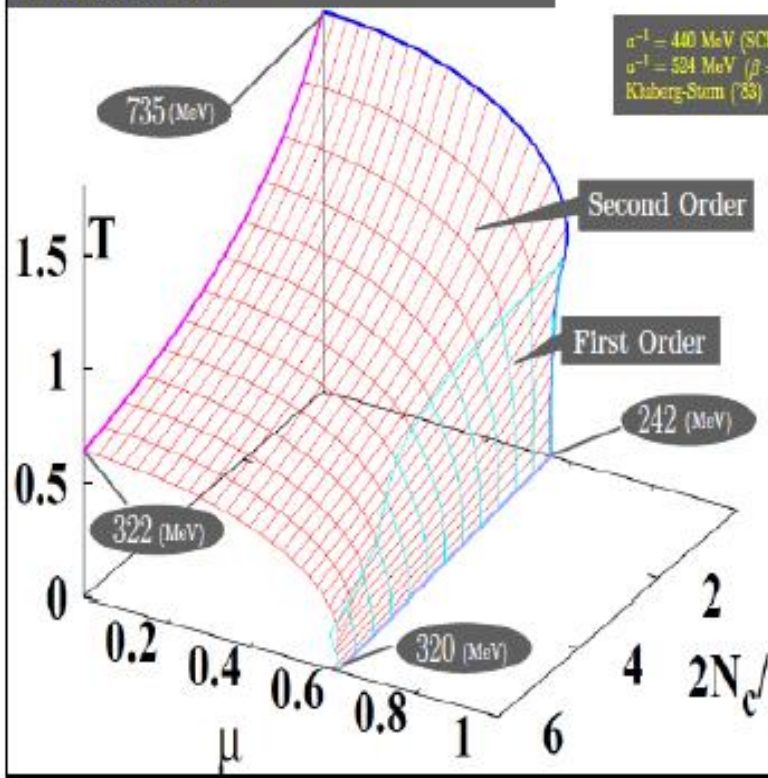
Phase Diagram Evolution with Increasing β
Next-to-Next-to-Leading Order of $1/g^2$ Expansion
arXiv:0911.3453, T-Z. Nakano, K. Miura and A. Ohnishi
Courtesy Kohtaroh Miura
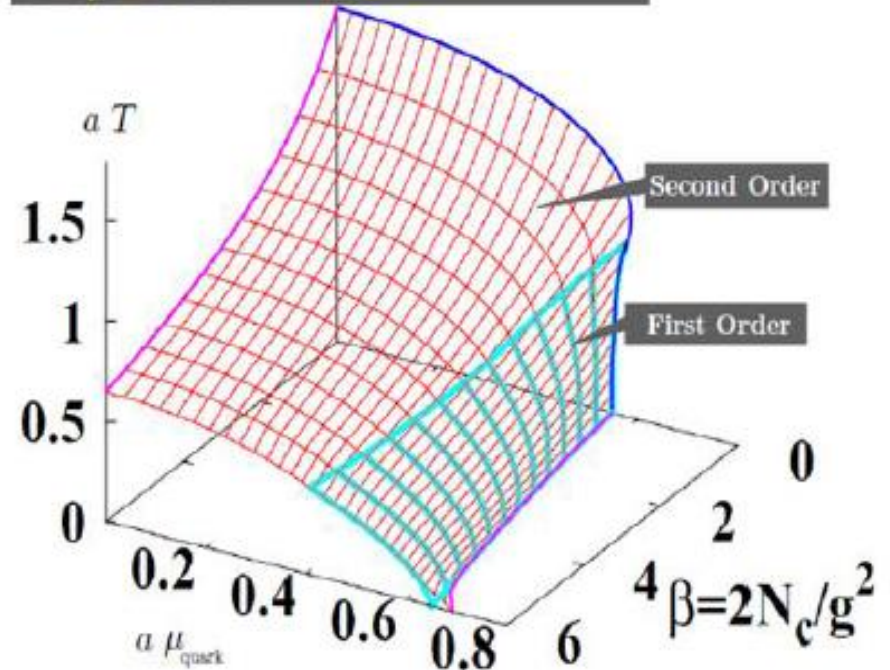
To be continued.....

TWO COLOR QCD

QCD with two colors

$$S_{kin} = \sum_{x, \nu=1,3} \frac{\eta_\nu(x)}{2} \left[\bar{\chi}(x)U_\nu(x)\chi(x+\hat{\nu}) - \bar{\chi}(x)U_\nu^\dagger(x-\hat{\nu})\chi(x-\hat{\nu}) \right]$$

$$+ \sum_x \frac{\eta_t(x)}{2} \left[\bar{\chi}(x)e^\mu U_t(x)\chi(x+\hat{t}) - \bar{\chi}(x)e^{-\mu}U_t^\dagger(x-\hat{t})\chi(x-\hat{t}) \right]$$

$$S_{kin} = \sum_{x\ even, \nu=1,3} \frac{\eta_\nu(x)}{2} \left[\bar{X}_e(x)U_\nu(x)X_o(x+\hat{\nu}) - \bar{X}_e(x)U_\nu^\dagger(x-\hat{\nu})X_o(x-\hat{\nu}) \right]$$

$$+ \sum_{x\ even} \frac{\eta_t(x)}{2} \left[\bar{X}_e(x) \begin{pmatrix} e^\mu & 0 \\ 0 & e^{-\mu} \end{pmatrix} U_t(x)X_o(x+\hat{t}) - - - - \right.$$

$$\left. \bar{X}_e(x) \begin{pmatrix} e^{-\mu} & 0 \\ 0 & e^\mu \end{pmatrix} U_t^\dagger(x-\hat{t})X_o(x-\hat{t}) \right]$$

$$\bar{X}_e = (\bar{\chi}_e, -\chi_e^{tr}\tau_2) \quad : \quad X_o = \begin{pmatrix} \chi_o \\ -\tau_2\bar{\chi}_o^{tr} \end{pmatrix}$$

Pauli—Gursey Symmetry: quarks and antiquarks transform according to equivalent reps.

Spectrum and condensates

Quark propagator
$$G_{ij} = \begin{pmatrix} a & b \\ -b^\star & a^\star \end{pmatrix}$$
SU(2) matrix

pion	$\mathrm{tr}GG^\dagger = (a^2 + b^2)$
scalar meson	$\varepsilon\mathrm{tr}GG^\dagger = \varepsilon(a^2 + b^2)$
scalar qq	$\det G = (a^2 + b^2)$
scalar $\bar{q}\bar{q}$	$\det G^\dagger = (a^2 + b^2)$
pseudoscalar qq	$\varepsilon\det G = \varepsilon(a^2 + b^2)$
pseudoscalar $\bar{q}\bar{q}$	$\varepsilon\det G^\dagger = \varepsilon(a^2 + b^2)$

Hands, Kogut, MpL, Morrison 1999

Mesons and Baryons are degenerate at T,μ=0

The degeneracy is lifted at T,μ ≠ 0

pion	$\mathrm{tr}G(\mu)G^\dagger(-\mu)$
scalar qq	$\det G(\mu)$

Rotation of condensates
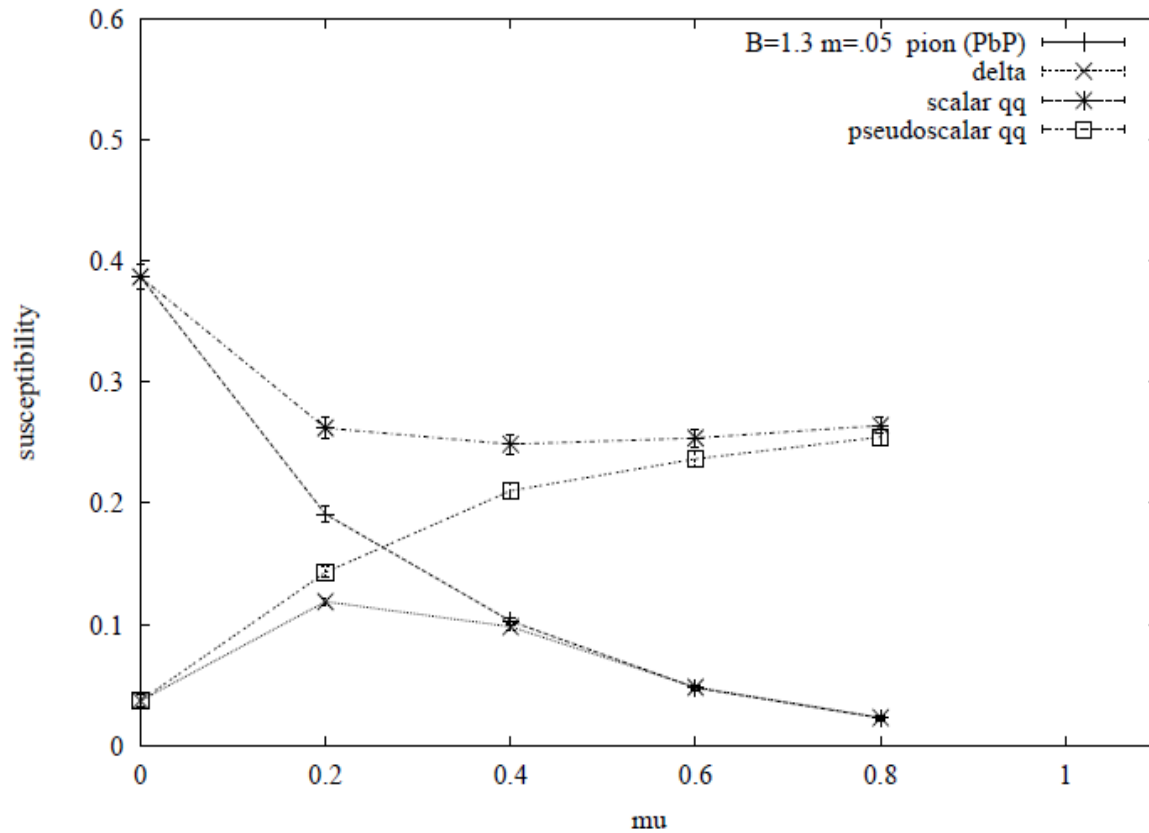
Quarkyonic phase – Two color
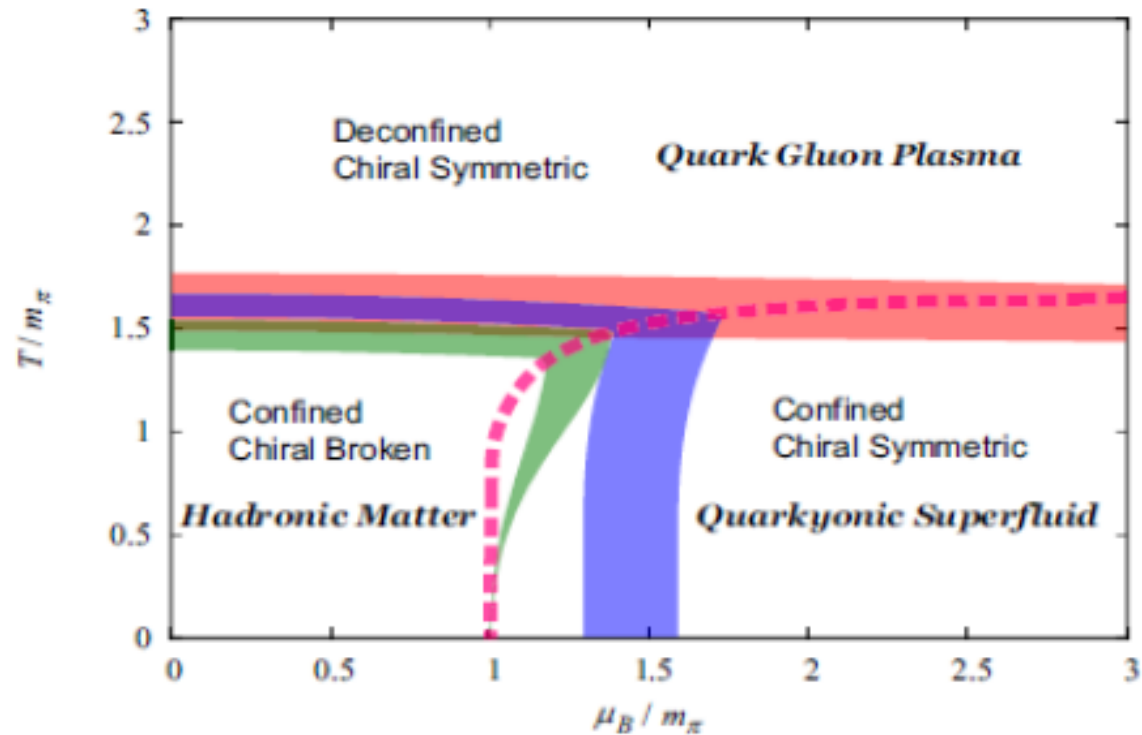
Brauner, Fukushima, Hidaka 2009

A Quarkyonic Phase in Dense Two Color Matter

Simon Hands

Department of Physics, Swansea University, Singleton Park, Swansea SA2 8PP, U.K.

Seyong Kim

Department of Physics, Sejong University, Seoul 143-747, Korea.

Jon-Ivar Skullerud

Department of Mathematical Physics, National University of Ireland Maynooth, Maynooth, County Kildare, Ireland.
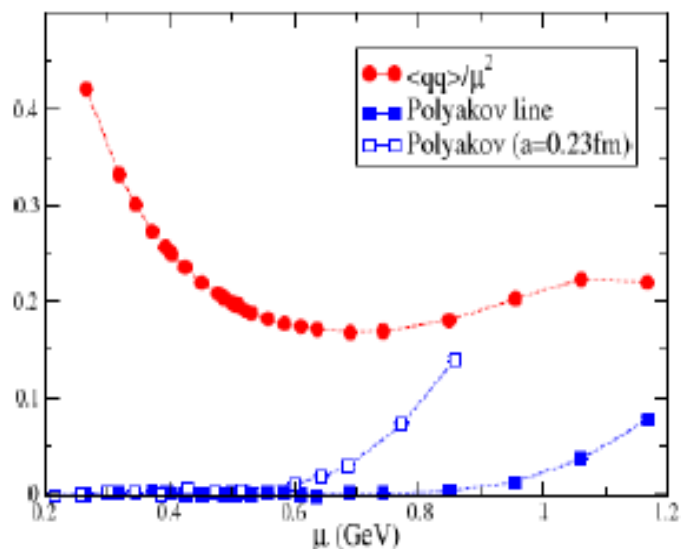
FIG. 4: (Color online) Superfluid order parameter $\langle qq \rangle / \mu^2$ and Polyakov line versus μ.
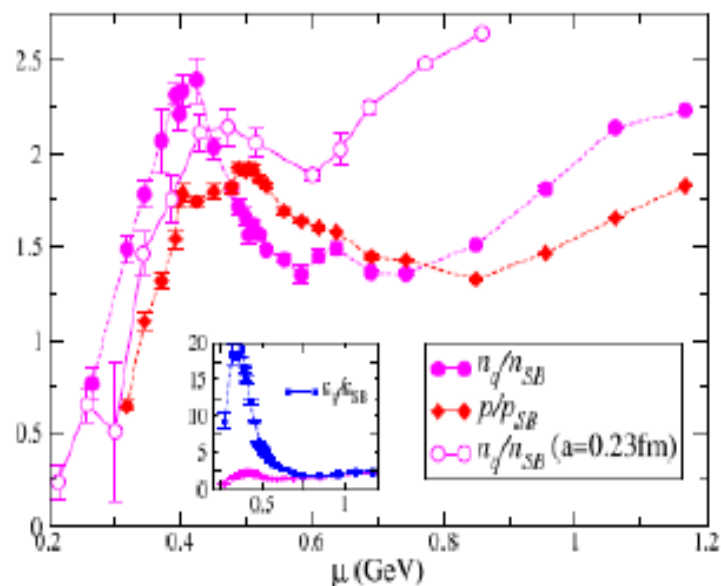
FIG. 1: (Color online) n_q/n_{SB} and p/p_{SB} vs. μ for QC$_2$D. Inset shows $\varepsilon_q/\varepsilon_{SB}$ for comparison.

Phases of two color QCD

Hands, Skullerud, Kim 2013
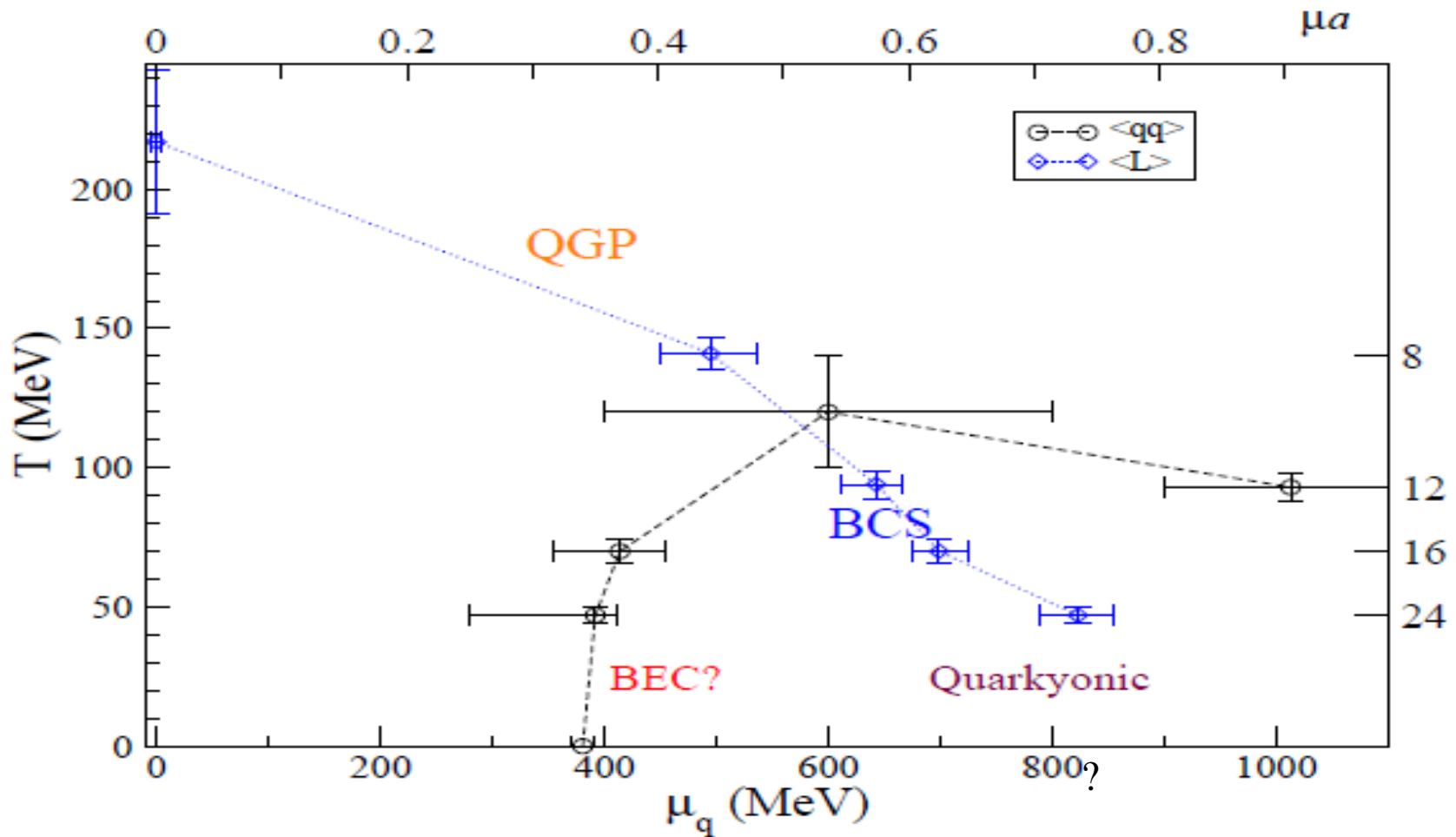
QCD

The sign problem

$$\mathcal{Z}(T, \mu, U) = \int dU e^{-(S_{YM}(U) - \log(\det M))}$$

$$M^{\dagger}(\mu_B) = -M(-\mu_B)$$

Complex for real μ

Possibilities for a real determinant:

$$M^{\dagger} = PMP^{-1} \qquad P = \gamma_5$$

Wilson fermions

Four fermion models

$$M^* = QMQ^{-1}$$

Imaginary

μ

$$M(\mu) = \begin{pmatrix} L(\mu) & 0 \\ 0 & L(-\mu) \end{pmatrix} \qquad L(\mu)^{\dagger} = \gamma_5 L(-\mu)\gamma_5$$

$$\det M(\mu) = |\det L(\mu)|^2 \geq 0.$$

Two color, isospin density

Features of the phase of the determinant

Summarizing:

- Quark mass outside eigenvalues: Gaussian

$$\langle\delta(\theta-\theta')\rangle = \frac{1}{\sqrt{\pi\Omega}}e^{-\theta^2/\Omega} \qquad \text{for} \qquad \mu < \mu_c,\ N_c \to \infty,$$

- Quark mass inside eigenvalues: Lorentzian

$$\langle\delta(2\theta-2\theta')\rangle = \frac{1}{\pi}\frac{\sinh(2nN_c\mu)}{\cosh(2nN_c\mu)-\cos(2\theta)} \qquad \text{for} \qquad \mu > \mu_c,\ 2\theta \in [-\pi,\pi].$$

MpL, Splittorff, Verbaarschot 2010
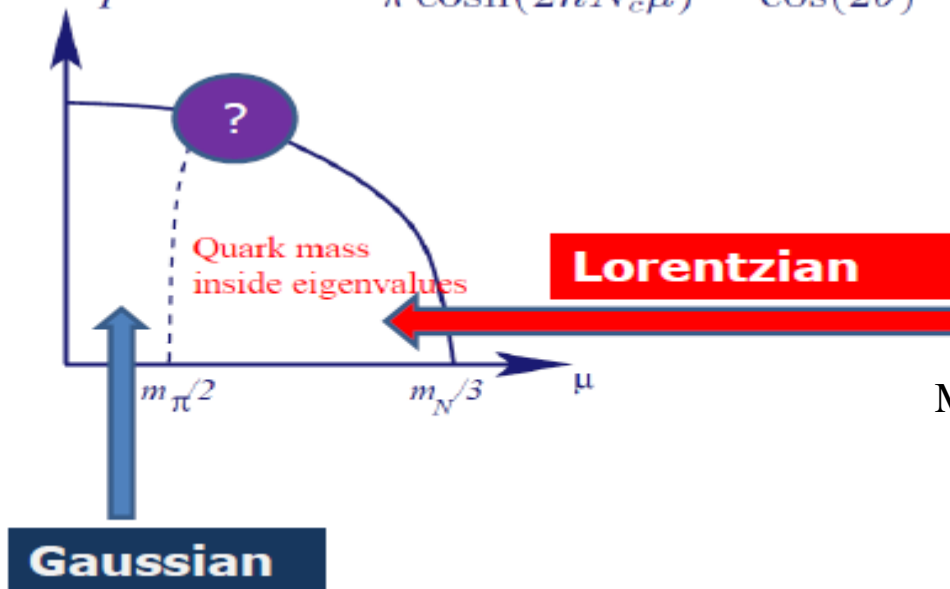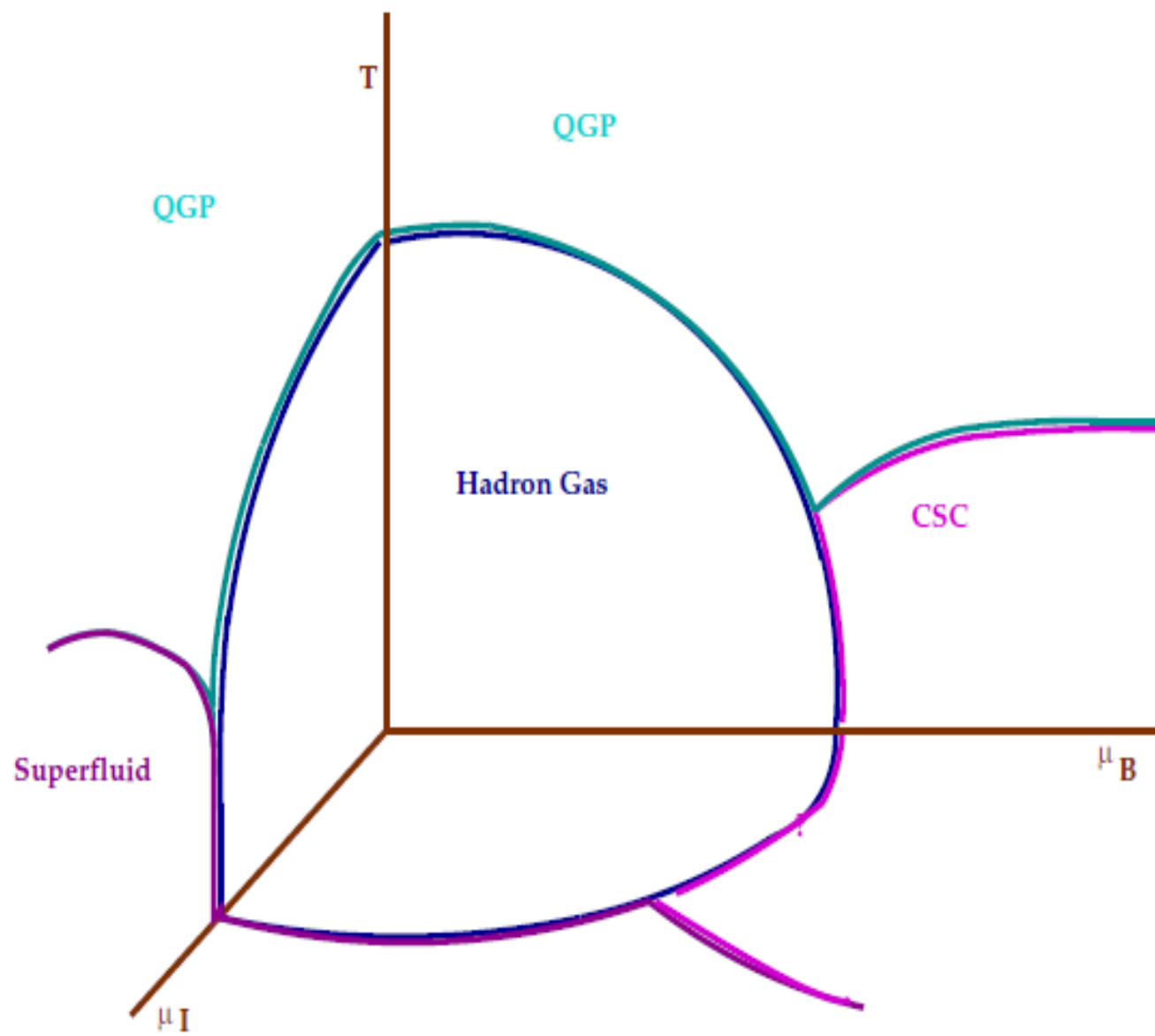
Because of the QCD symmetries, the complex μ_B plane

Complex μ Plane

Im μ

Real μ
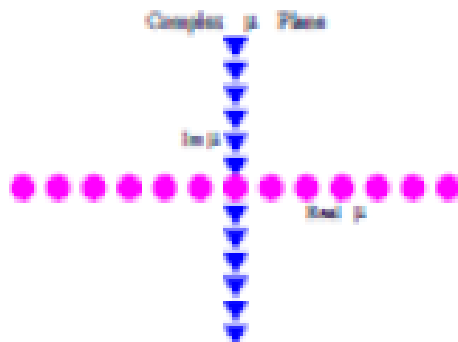
can be mapped onto the complex μ_B^2 plane

Complex μ^2 Plane

Im μ

Real μ

Useful to consider the QCD phase diagram in the temperature, μ^2 plane
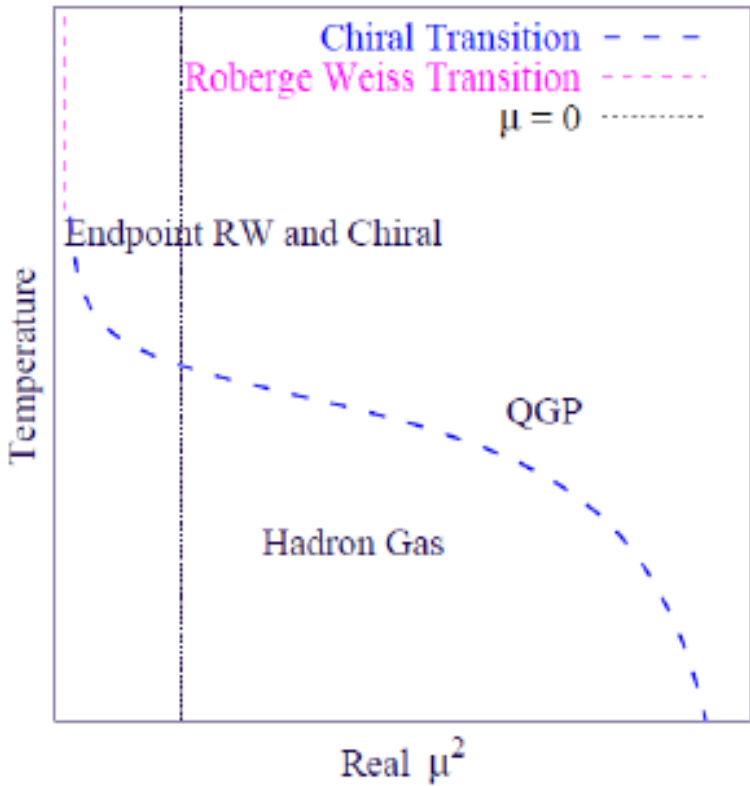
Imaginary chemical potential

- **Imaginary chemical potential: main problem, control over analytic continuation**
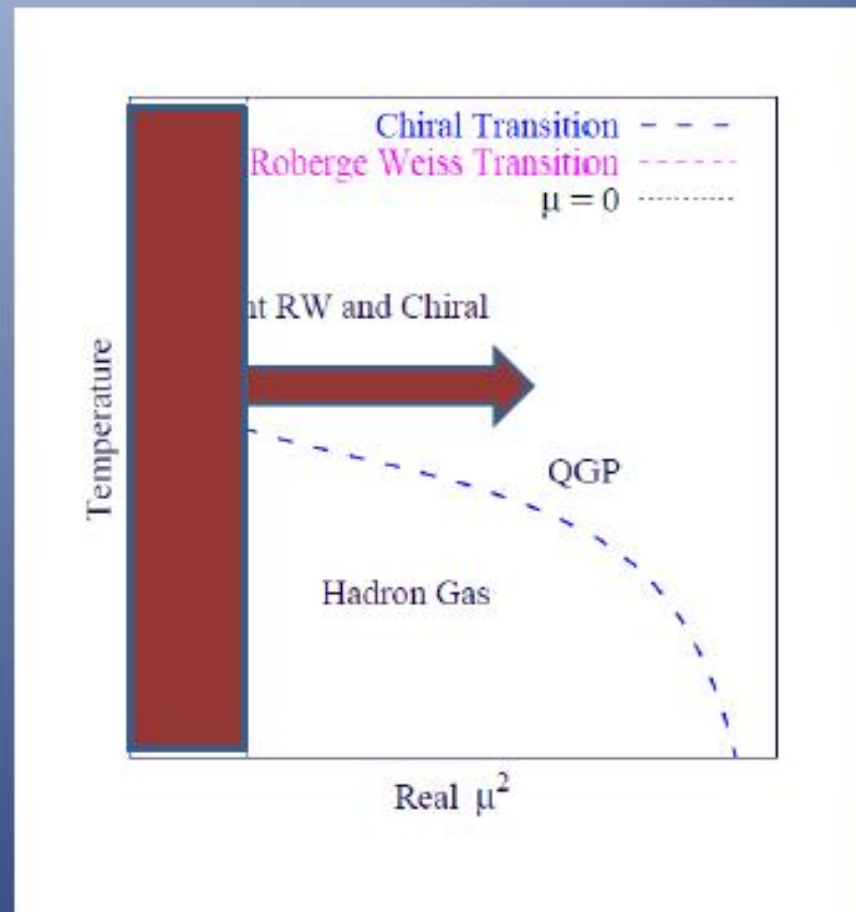
Taylor expansion

- **Taylor expansion: main problem, control of the convergence**
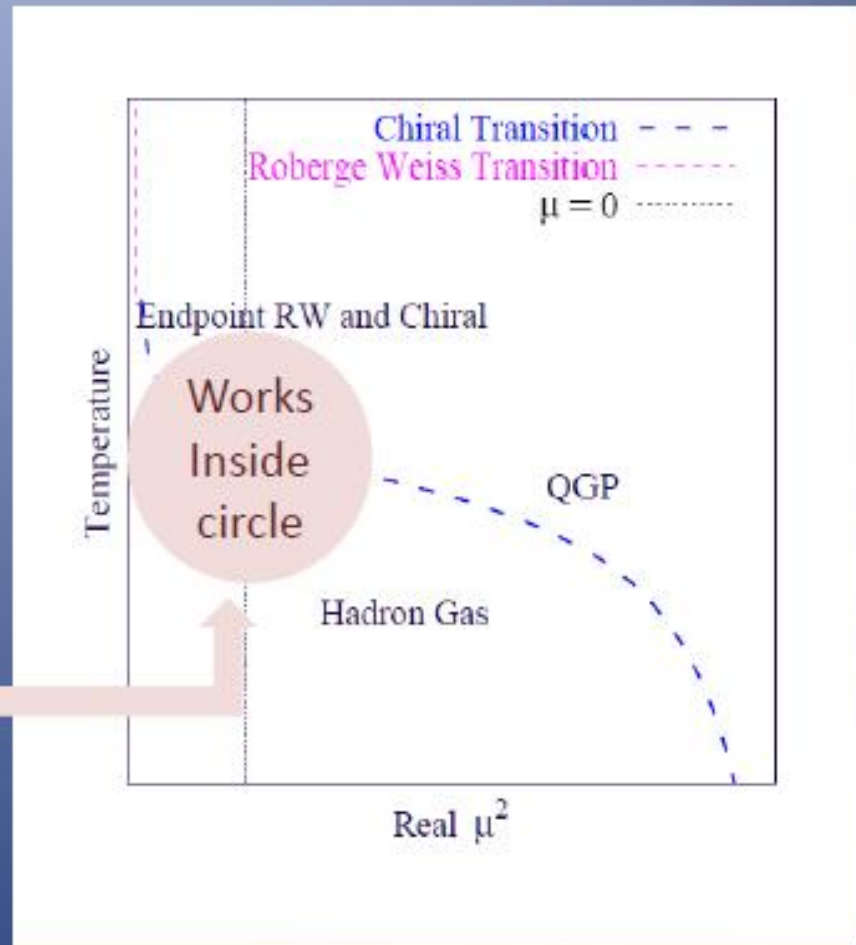
All methods work at high T
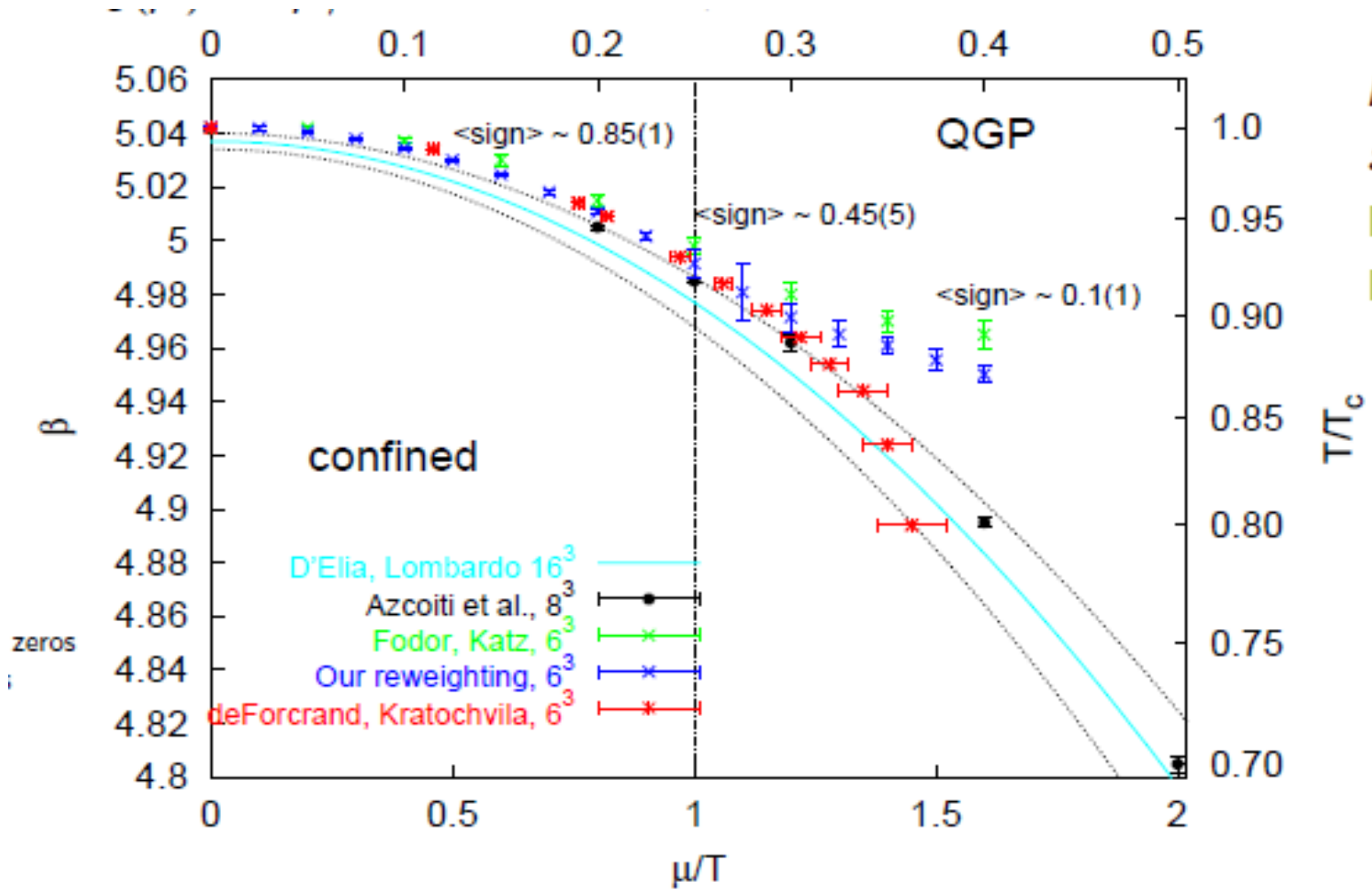
SEARCHING FOR THE QCD CRITICAL POINT

STRATEGY II : GAVAI AND GUPTA, BIELEFELD-RBC

Series expansion for the pressure:

$$P(T, \mu_B) = P(T) + \frac{1}{2}\chi_B^{(2)}(T)\mu_B^2 + \frac{1}{4!}\chi_B^{(4)}(T)\mu_B^4 + \frac{1}{6!}\chi_B^{(6)}(T)\mu_B^6 + \frac{1}{8!}\chi_B^{(8)}(T)\mu_B^8 + \cdots,$$

The quark number susceptibility has the expansion

$$\chi_B(T, \mu_B) = \chi_B^{(2)}(T) + \frac{1}{2}\chi_B^{(4)}(T)\mu_B^2 + \frac{1}{4!}\chi_B^{(6)}(T)\mu_B^4 + \frac{1}{6!}\chi_B^{(8)}(T)\mu_B^6 + \cdots.$$

THIS SERIES IS EXPECTED TO DIVERGE AT THE QCD CRITICAL END POINT.   RADIUS OF CONVERGENCE IS

$$\lim_{n \to \infty} \mu_*^{(n)} = \sqrt{\frac{1}{n(n-1)} \frac{\chi_B^{(n+2)}}{\chi_B^{(n)}}}.$$

The endpoint is the first singularity in the complex μ plane occurring at real μ.
Coefficients should be all positive at large n

Back to the complex μ plane

Singularities for complex μ
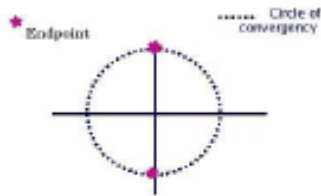
Endpoint of the RW Transition
$T_R > T_c$

Endpoint of the Chiral Transition
$T_\chi < T_c$
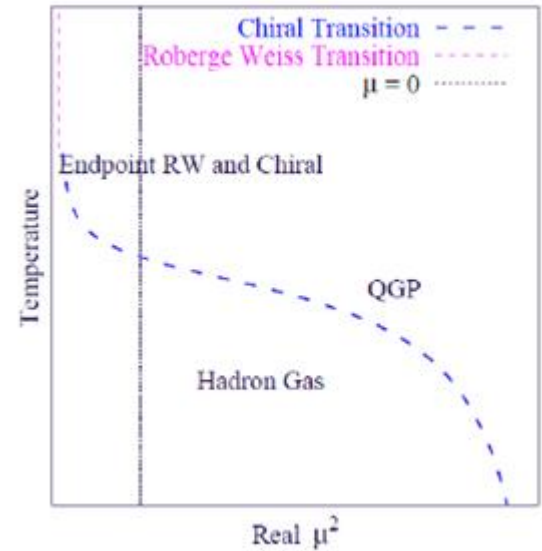
The radius of convergence (?)
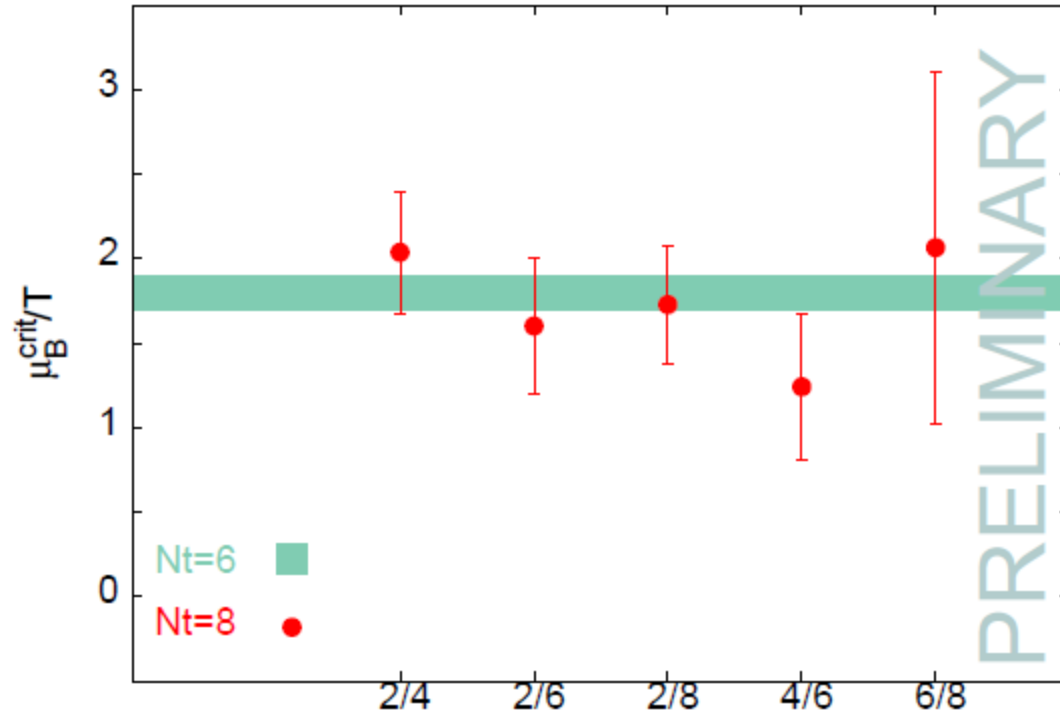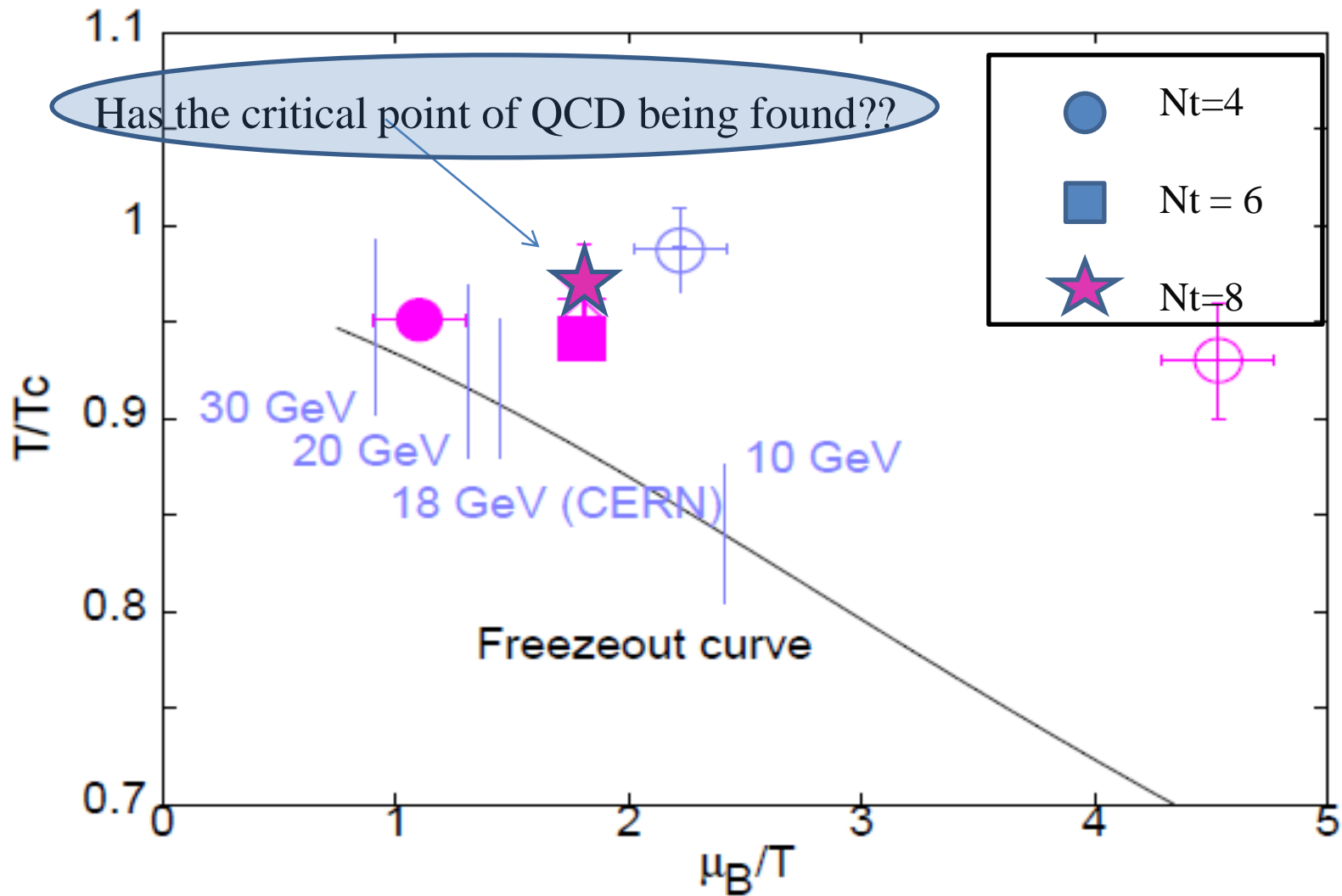
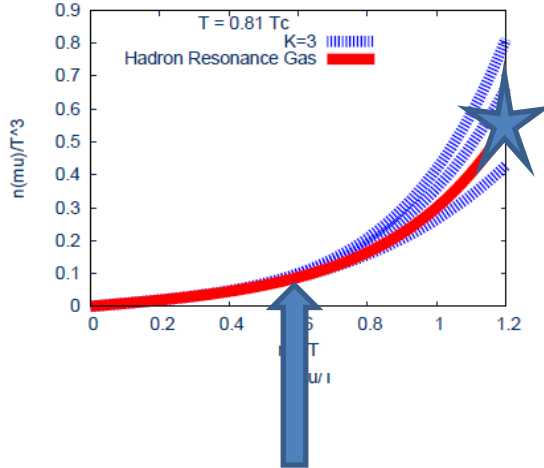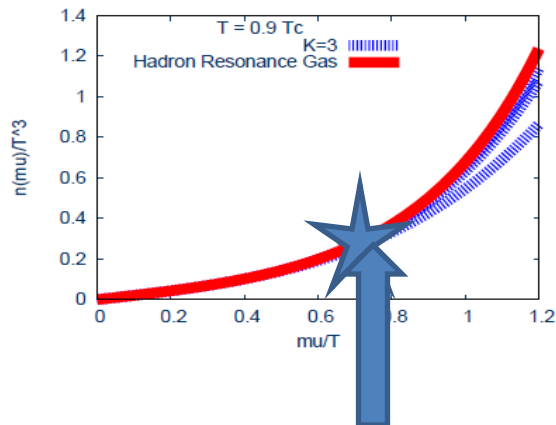# Lower bound on the radius of convergence And freezout point

T = 0.81 Tc

T = 0.87 Tc

★ Freezout point
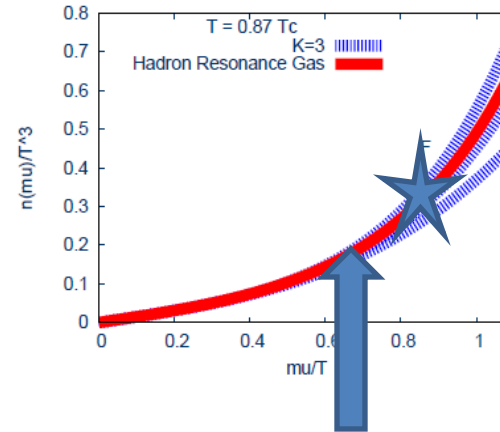
T = 0.90 Tc

T = 0.96 Tc
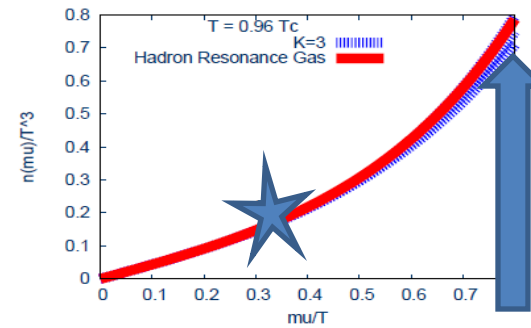
# Use imaginary μ to validate radius of convergence

Falcone, Meyer, Laermann, MpL

Chiral Transition – – –
Roberge Weiss Transition – – – – –
$\mu = 0$ ···········

Endpoint RW and Chiral

Candidate
Critical point
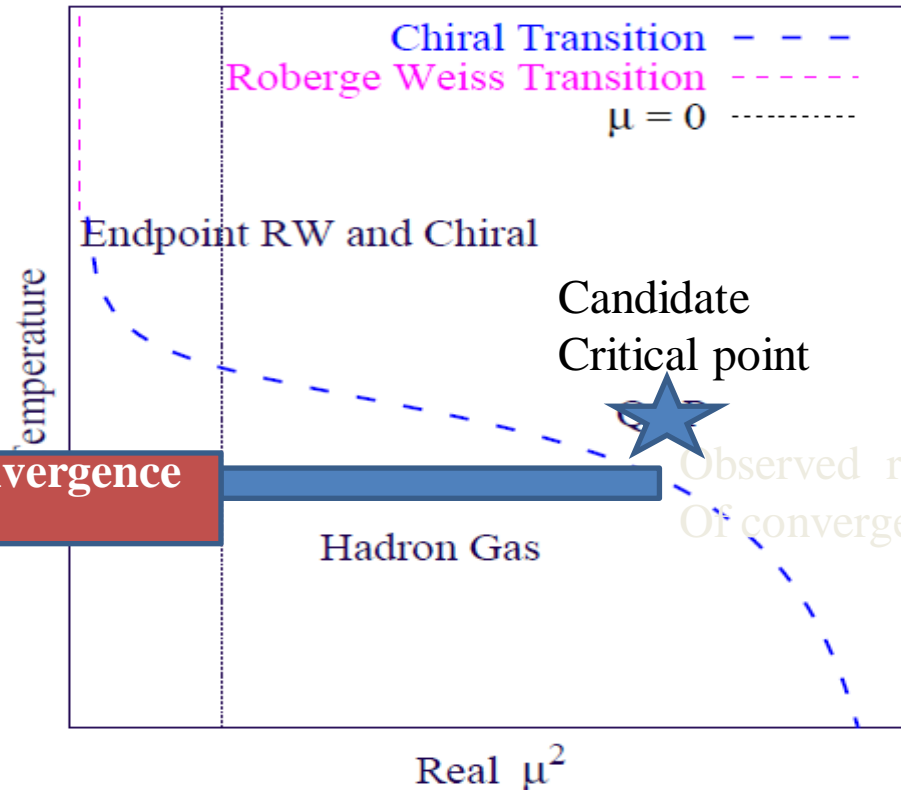
Check radius of convergence here!

Observed radius
Of convergence

Temperature

Hadron Gas

Real μ^2

Alternative estimate of the radius of convergence

Laermann, MpL, Meyer 2013

Falcone, Laermann, Meyer, MpL
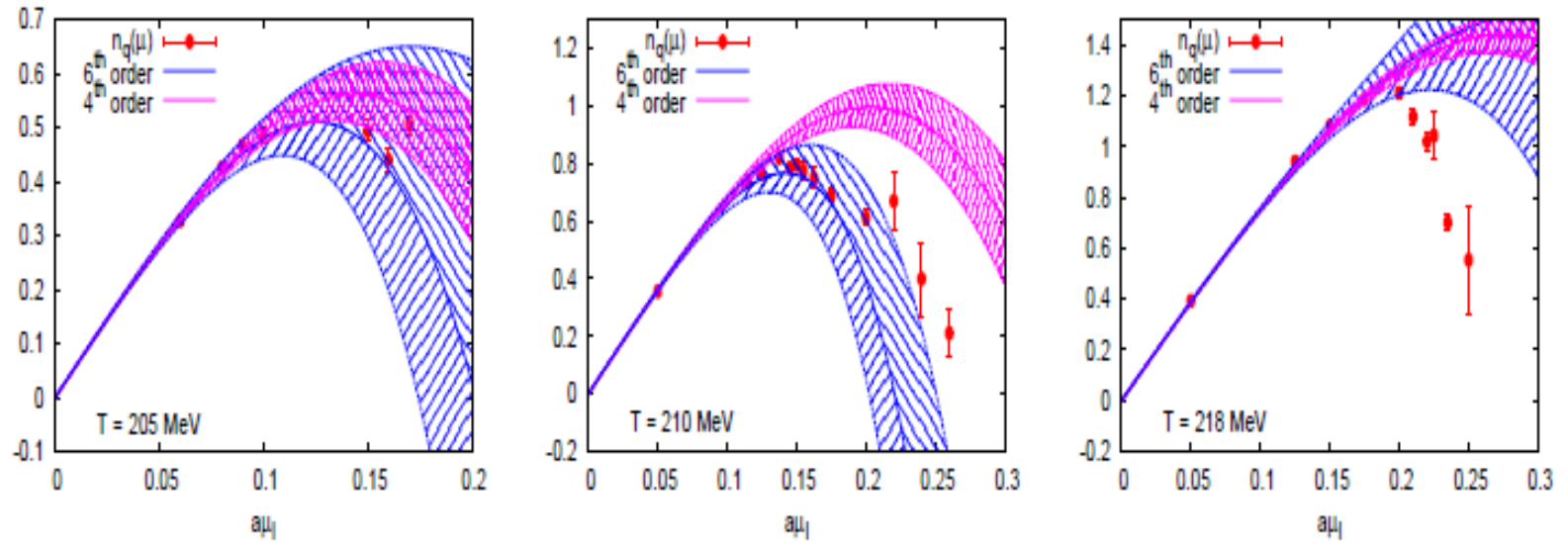
A proposal for a better control on the QCD critical point

US NSAC Long RangePlan (adapted)